1 **Hypothalamic estrogen receptor alpha mediates key side effects of tamoxifen therapy in**

2 **mice**

3 Zhang, Z[1,2], Park, J. W.[1,2], Ahn, I. S., Diamante[1], G., Sivakumar, N.[1], Arneson, D. V., Yang, X.[1],

4 van Veen, J. E.[1,2#] and Correa, S. M.[1,2#]

5

6 Affiliations

7 [1] Department of Integrative Biology and Physiology

8 [2] Laboratory of Neuroendocrinology of the Brain Research Institute

9 University of California, Los Angeles, CA, USA

10

11 [#]Authors for correspondence: stephaniecorrea@ucla.edu and vanveen@ucla.edu

12

13

14

15

16

17 Keywords: tamoxifen, hypothalamus, estrogen receptor alpha, thermoregulation, hot flashes,

18 physical activity, bone

19

20

Abstract

Adjuvant tamoxifen therapy for invasive breast cancer improves patient survival. Unfortunately, long-term treatment comes with side effects that impact health and quality of life, including hot flashes, changes in bone density, and fatigue. Partly due to a lack of proven animal models, the tissues and cell types that mediate these negative side effects are largely unknown. Here we show that mice undergoing a 28-day course of tamoxifen treatment experience dysregulation of core and skin temperature, changes in bone density, and decreased physical activity, recapitulating key aspects of the human physiological response. Single cell RNA sequencing reveals that tamoxifen treatment induces significant and widespread gene expression changes in different cell types of the hypothalamus, most strongly in neurons and ependymal cells. These expression changes are dependent on estrogen receptor alpha (ERα), as conditional knockout of ERα in the hypothalamus ablated or reversed tamoxifen-induced gene expression. Accordingly, ERα-deficient mice do not exhibit changes in thermal regulation, bone density, or movement in response to tamoxifen treatment. These findings provide mechanistic insight into the effects of tamoxifen on the hypothalamus and support a model in which hypothalamic ERα mediates several key side effects of tamoxifen therapy.

Introduction

Tamoxifen is a selective estrogen receptor modulator that has been used for effective treatment of hormone responsive breast cancers for more than 40 years *(Jordan 2003)*. As an adjuvant, tamoxifen therapy can decrease the incidence of breast cancer recurrence by up to 40 percent *(Davies et al. 2011)*. This exceptionally effective treatment remains standard of care for people with hormone-responsive cancers, and reduction of recurrence persists for at least ten years of continuous tamoxifen treatment *(Davies et al. 2013, Chlebowski et al. 2014, Gierach et al. 2017)*. In contrast to these benefits, tamoxifen treatment has been associated with a variety of

46   negative side effects including increased risk for hot flashes*(Love et al. 1991, Howell et al. 2005,*

47   *Francis et al. 2015)*, endometrial cancer, venous thromboembolic events *(Fisher et al. 1998,*

48   *Cuzick et al. 2007)*, bone loss *(Powles et al. 1996)*, and fatigue *(Haghighat et al. 2003)*. These

49   responses markedly impact quality of life. Accordingly, ~25% of eligible patients fail to start or

50   complete this life-saving therapy due to side effects and safety concerns *(Friese et al. 2013,*

51   *Berkowitz et al. 2020)*. The tissues and cells that mediate these negative side effects remain

52   unclear. Unraveling the cells and mechanisms that mediate the positive effects of tamoxifen from

53   those that mediate the negative side effects is necessary for understanding the multifaceted

54   effects of tamoxifen therapy on physiology. Ultimately, this knowledge could lead to the design of

55   new or adjuvant therapies that circumvent the side effects, improve patient quality of life, and

56   perhaps enhance survival via increased patient compliance.

57   Within the brain, the hypothalamus is highly enriched for estrogen receptor expression

58   and represents an excellent anatomical candidate for mediating many of the side effects of

59   tamoxifen therapy. Estrogen receptor alpha (ERα) signaling regulates body temperature *(Bowe*

60   *et al. 2006, Musatov et al. 2007, Mittelman-Smith et al. 2012, Martinez de Morentin et al. 2014)*,

61   physical activity *(Musatov et al. 2007, Correa et al. 2015, van Veen et al. 2020)*, and bone density

62   *(Farman et al. 2016, Zhang et al. 2016, Herber et al. 2019)* through distinct neuron populations in

63   the hypothalamus. Indeed, the hypothalamus is a demonstrated target of tamoxifen, leading to

64   changes in food intake and body weight *(Wade et al. 1993, Lopez et al. 2006, Lampert et al. 2013)*

65   and changes in the hypothalamic-pituitary-ovarian *(Wilson et al. 2003, Aquino et al. 2016)* and

66   hypothalamic-pituitary-adrenal *(Wilson et al. 2003)* axes. Tamoxifen has also been shown to

67   affect gene expression in the hypothalamus; its administration blocks the estrogen dependent

68   induction of the progesterone receptor (*Pgr*) in the ventromedial hypothalamus (VMH) and

69   increases the expression of estrogen receptor beta (*Esr2*) in the paraventricular nucleus of the

70   hypothalamus (PVH) *(Patisaul et al. 2003, Aquino et al. 2016, Sa et al. 2016)*.

71 We hypothesized that tamoxifen alters estrogen receptor signaling in the hypothalamus to

72 mediate key negative side effects of tamoxifen therapy. To test this hypothesis, we modeled

73 tamoxifen therapy in mice with a 28-day treatment course based on human dosage *(Slee et al.*

74 *1988)* and asked if mice experience physiological effects similar to humans. We measured

75 physical activity, bone density, and the temperature of the body core, tail skin, and thermogenic

76 brown adipose tissue (BAT). Profiling genome-wide expression changes of individual cells in the

77 hypothalamus using Drop-seq, a droplet-based single-cell RNA sequencing technology, revealed

78 transcriptional changes induced by tamoxifen in multiple cell types. Finally, we show that

79 hypothalamic ERα signaling is necessary for both the gene expression changes in the

80 hypothalamus and the effects on thermoregulation, bone density, and physical activity. Together,

81 these findings suggest that tamoxifen therapy modulates hypothalamic ERα signaling to alter

82 fundamental aspects of physiology and health. Dissecting central versus peripheral effects and

83 mechanisms of tamoxifen therapy is the first step toward identifying strategies to mitigate the

84 adverse side effects of this life-saving treatment.

85

86 **Results**

87 **Tamoxifen treatment alters thermoregulation.**

88 To ask if mice and humans experience similar physiological effects while under tamoxifen

89 treatment, we administered tamoxifen (0.1mg/kg) or vehicle subcutaneously, daily, for 4 weeks

90 (Figure 1A). In humans, hot flashes are characterized by frequent and sudden increases of heat

91 dissipation from the face and other parts of the skin, often accompanied with perspiration and a

92 decrease in core body temperature *(Stearns et al. 2002)*. Similarly, tamoxifen treated mice

93 showed significantly lower core body temperature compared to controls, as indicated by 24-hour

94 averages from the last week of treatment. This difference is detected during the light phase when

95 the animals are generally inactive but not in the dark phase when physical activity can also

96 influence core temperature (Figure 1B and C). In mice, heat dissipation occurs effectively via
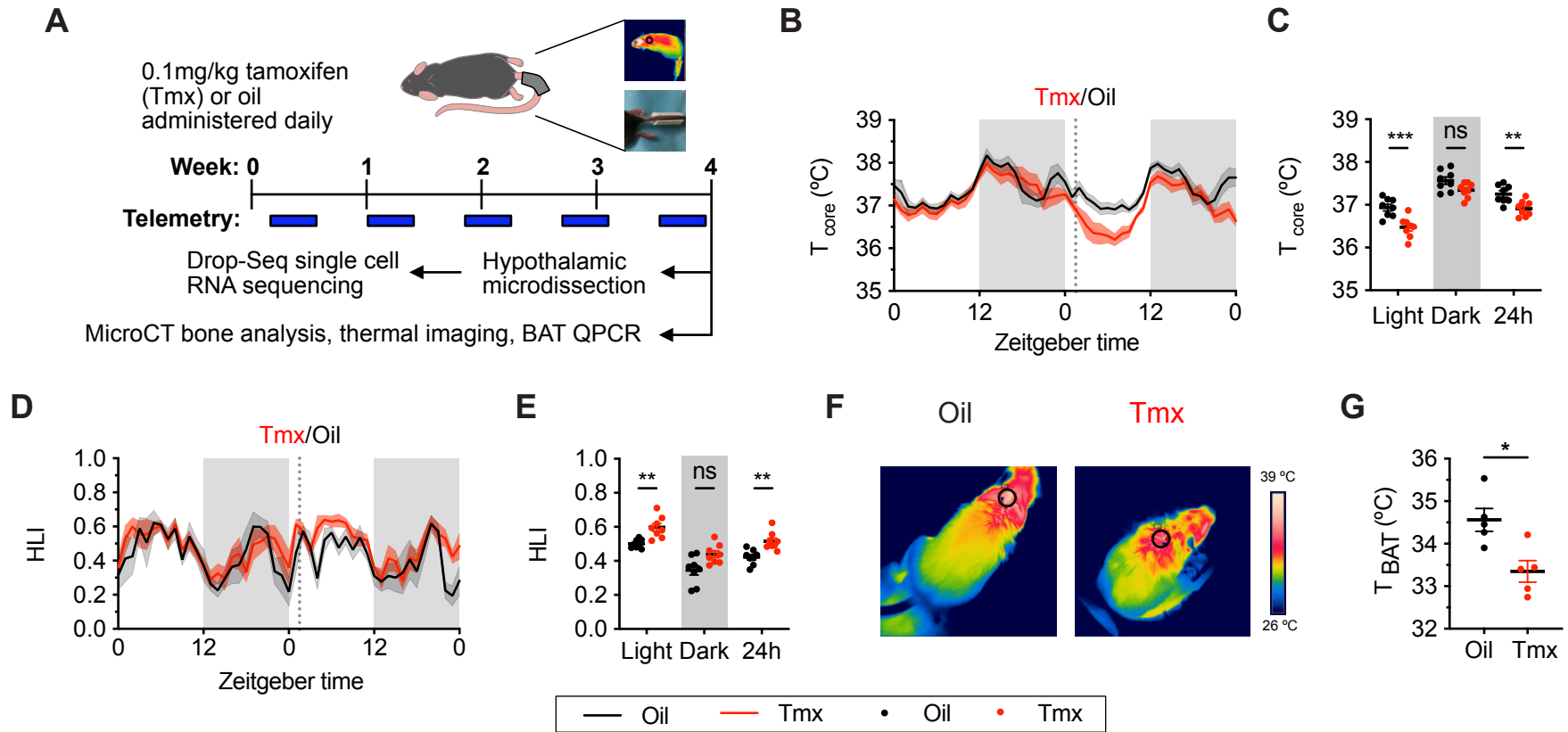
Zhang et al. Figure 1

Figure 1. Tamoxifen treatment decreases core body temperature and increases heat dissipation

(**A**) Strategy to measure the physiological and gene expression effects of long term tamoxifen (Tmx) treatment. Mice were treated by daily subcutaneous injection of 0.1mg/kg tamoxifen or corn oil for 4 weeks. Core and tail temperature were measured every 5 minutes using telemetry probes. Snap shot of thermographic images for BAT temperature was obtained in last week of treatment. At the conclusion of 4 week treatment, experimental mice were sacrificed for bone analysis or single cell RNA sequencing. (**B**) Hourly average of core body temperature over 3 days before and 3 weeks after injections (dotted line). (**C**) Average core body temperature from mice shown in panel **B** highlighting per animal averages in light (7:00 to 19:00), dark (19:00 to 7:00), and total 24 h periods (n=8, treatment **) (**D**) Heat loss index (HLI) calculated from continuous measurements of core and tail temperature. (**E**) Average HLI from mice shown in panel **D** (n=7, treatment **). (**F**) Thermographic images of interscapular skin above brown adipose tissues depots in mice injected with either oil or tamoxifen. (G) Quantification of temperature of skin above interscapular BAT depots (n=5). In **B** and **D**, line shading width represents SEM. *, P<0.05; **, P<0.01; ***, P<0.001 for Sidak's multiple comparison tests (**C** and **E**) following a significant effect of treatment in a two-way RM ANOVA or two tailed t-tests (**G**).

97   vasodilation in the tail *(Gordon 1993)*. As tail skin temperature is highly dependent on core and

98   ambient temperature, heat loss is often expressed as the heat loss index (HLI): HLI = (Tskin −

99   Tambient)/(Tcore − Tambient) *(Romanovsky et al. 2002)*. We observed a higher HLI in mice

100   treated with tamoxifen compared to controls (Figure 1D). Again, this effect was detected in the

101   light phase but not in the dark phase (Figure 1E). Tail skin temperature also was significantly

102   higher in tamoxifen treated mice compared to controls during light phase (Figure 1 – Supplement

103   1A and B). In addition, mice treated with tamoxifen exhibited lower temperature above the

104   intrascapular region directly apposed to BAT depots (Figure 1F and G), suggesting reduced heat

105   production from BAT following tamoxifen treatment. Accordingly, postmortem qPCR analysis of

106   BAT revealed lower expression of genes associated with thermogenesis, uncoupling protein 1

107   (*Ucp1*) and adrenergic receptor beta 3 (*Adrb3*) (Figure 1 – Supplement 1C), suggesting

108   suppressed BAT thermogenesis and sympathetic tone following tamoxifen treatment *(Cannon et*

109   *al. 2004)*. Together, these results indicate that tamoxifen treatment shifts mouse temperature

110   balance toward increased heat dissipation and decreased heat production, consistent with the

111   observations in humans experiencing hot flashes.

112

113   **Tamoxifen treatment increases bone density and decreases movement.**

114   Tamoxifen has been shown to affect bone density in rodent and human studies *(Powles*

115   *et al. 1996, Perry et al. 2005)*. Here, micro CT scans revealed that tamoxifen treatment is

116   associated with greater bone volume ratios in both metaphysis and diaphysis of the femur (Figure

117   2A-C). Tamoxifen treatment was also associated with greater number and thickness, and less

118   separation of trabecular bones in metaphysis (Figure 2B). Bone mineral density and bone area in

119   cortical bones were not significantly affected by tamoxifen treatment (Figure 2C); however,

120   tamoxifen treatment was associated with significantly greater cortical thickness (Figure 2A and

121   C). Together, these data indicate that chronic tamoxifen treatment increases bone mass,

122   consistent with previous studies showing increased bone formation and bone mass in mice
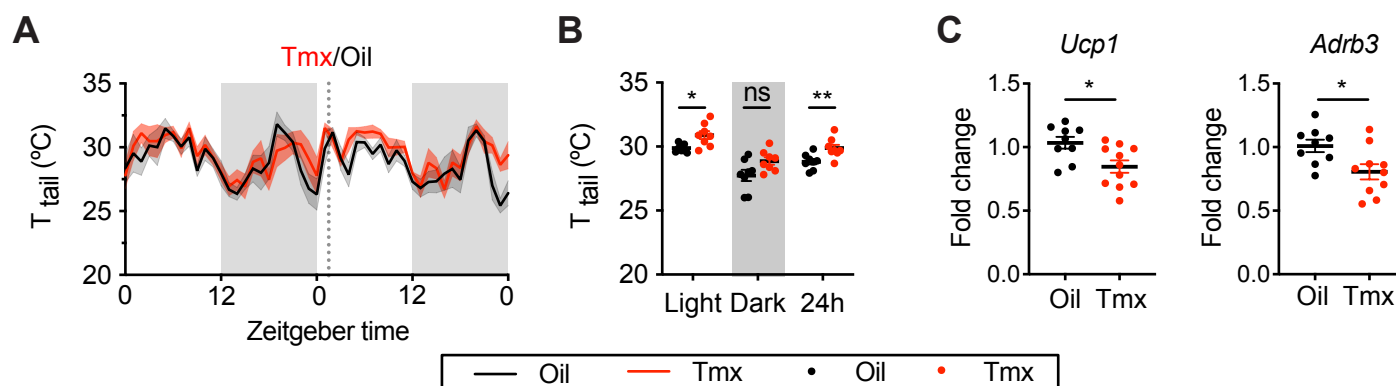
Figure 1 - Supplement 1 - Tamoxifen increased temperature in tail and suppressed thermogenic gene expression in BAT.

(**A**) Hourly average of tail skin temperature over 3 days before and 3 weeks after injections (dotted line) measured every 5 min using attached thermal logger. (**B**) Average tail temperature from mice shown in panel **A** highlighting per animal averages in light, dark, and total 24 h periods (n=8, treatment **). (**C**) Relative mRNA expression of *Ucp1* and *Adrb3* from BAT extracts (n=8-10). ns, non-significant; *, P<0.05; **, P<0.01 for Sidak's multiple comparison tests (**B**) following a significant effect of treatment in a two-way RM ANOVA or two tailed t-tests (**C**).
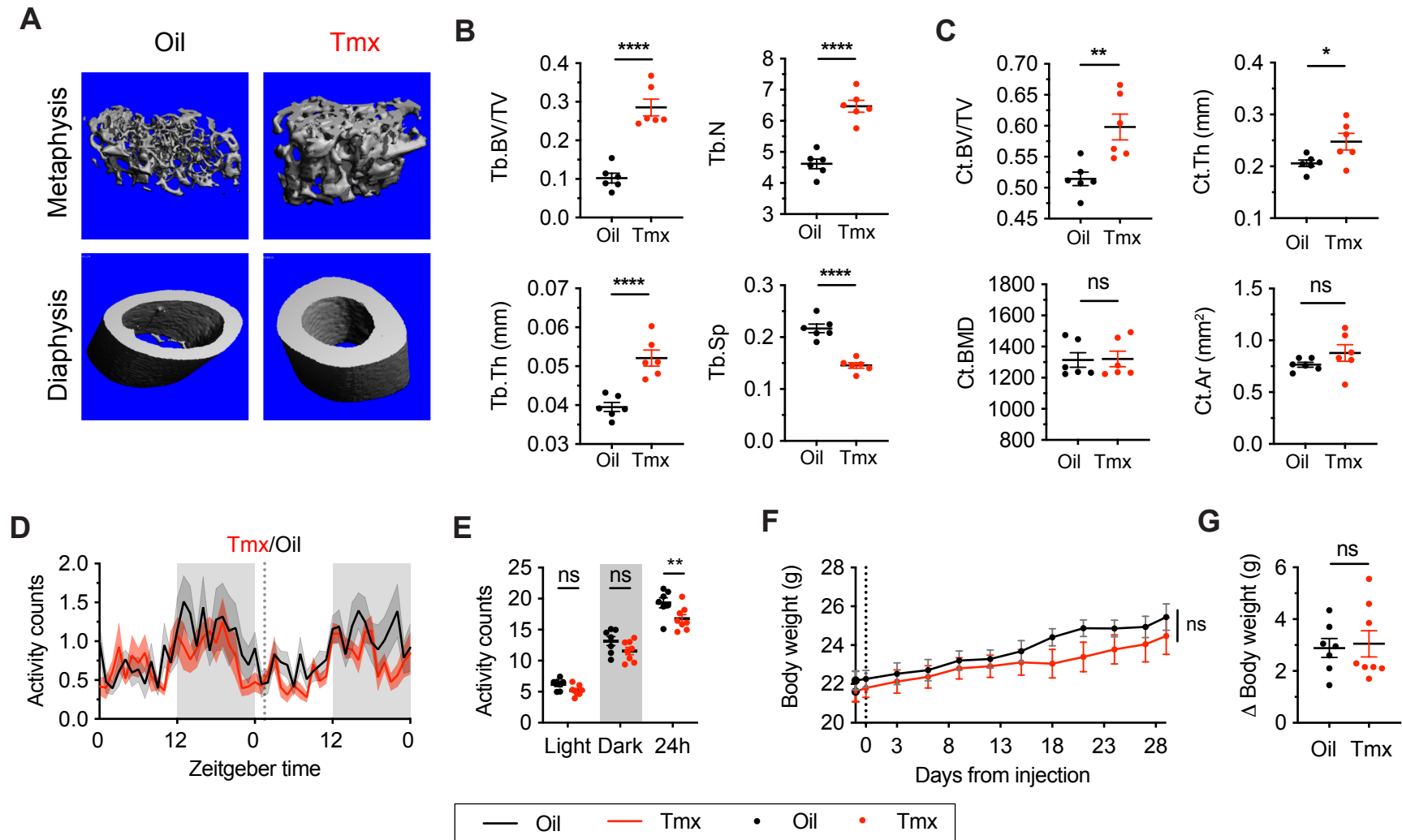
Figure 2. Tamoxifen treatment increases bone density and decreases movement.

(**A**) Representative microCT images showing bone density of the distal metaphysis and midshaft diaphysis of femurs from tamoxifen or oil treated female mice. Tamoxifen or vehicle was injected subcutaneously at 0.1mg/kg for 28 days. (**B**) Trabecular bone volume fraction (BV/TV), trabecular numbers (Tb.N), trabecular thickness (Tb.Th) and trabecular separation (Tb.Sp) in distal metaphysis of femurs (n=6). (**C**) Bone volume fraction (Ct.BV/TV), cortical thickness (Ct.Th), bone mineral density (Ct.BMD) and cortical area (Ct.Ar) in diaphysis of femurs (n=6). (**D**) Hourly average of physical activity over 3 days before and 3 weeks after tamoxifen or oil injections (dotted line) measured every 5 min using intraperitoneous telemetry probe. Line shading width represents SEM. (**E**) Average total physical activity from mice shown in panel **D** (n=8, treatment *). (**F**) Change of body weight over 28 days during tamoxifen or oil injection (n=7-8, treatment P=0.5468). Error bars represent SEM. (**G**) total change in body weight over the course of the 28 day experiment (n=8, P=0.8010). ns, non-significant; **, P<0.01; ***, P<0.001; ****, P<0.0001 for Sidak's multiple comparison tests (**E**) following a significant effect of treatment in a two-way RM ANOVA or two tailed t-tests (**B**, **C** and **G**).

123   following tamoxifen administration *(Perry et al. 2005, Starnes et al. 2007)*. In addition, tamoxifen

124   resulted in a moderate decrease in 24 h physical activity (Figure 2D and E). Tamoxifen treated

125   mice did not show significant changes in body weight compared to control mice, over 28 days of

126   treatment (Figure 2F and G).

127

128   **Tamoxifen administration affects gene expression in all hypothalamic cell types**

129   To ask how tamoxifen affects gene expression in the different cell types of the

130   hypothalamus, we collected hypothalami (Figure 3 – Supplement 1A) after 28 daily injections of

131   tamoxifen or vehicle and analyzed individual cells by drop-Seq *(Macosko et al. 2015)*. A total of

132   29,807 cells (8,220 from n = 3 vehicle treated mice, 21,587 from n = 5 tamoxifen treated mice)

133   clustered into 9 distinct cell types, annotated based on high expression of previously

134   characterized cell type markers *(Moffitt et al. 2018, Saunders et al. 2018)*: astrocytes,

135   oligodendrocytes, neurons, endothelial cells, microglia, polydendrocytes, ependymal cells, mural

136   cells, and fibroblasts (UMAP: Figure 3A, tSNE: Figure 3 – Supplement 1B, cluster defining marker

137   expression: Figure 3 – Supplement 1D). Because tamoxifen modulates estrogen receptor

138   signaling *(de Médina et al. 2004, Jordan 2007)*, we examined cell-type specific expression of

139   three estrogen receptor transcripts: the nuclear receptors *Esr1* and *Esr2,* as well as the G-protein-

140   coupled estrogen receptor 1 (*Gper1,* formerly *Gpr30*) *(Revankar et al. 2005)*. While neither *Esr1*,

141   *Esr2*, or the *Esr1* target gene *Pgr* showed strong enrichment in any particular cell type (Figure

142   3B), *Gper1* transcripts were predominantly found in Mural cells (LogFC: 1.39 compared to all

143   other cell types, adj. P < 1e-128). These results are in accordance with the reported *Esr1*

144   expression pattern in the hypothalamus *(Shughrue et al. 1997)* and *Gper1* in vascular smooth

145   muscle of the rodent brain *(Isensee et al. 2009)*. The graphical clustering methods, UMAP and

146   tSNE did not demonstrate clear separation between tamoxifen and vehicle treated cells (Figure

147   3C, Figure 3 – Supplement 1C), indicating that the effect of tamoxifen at clinically relevant doses

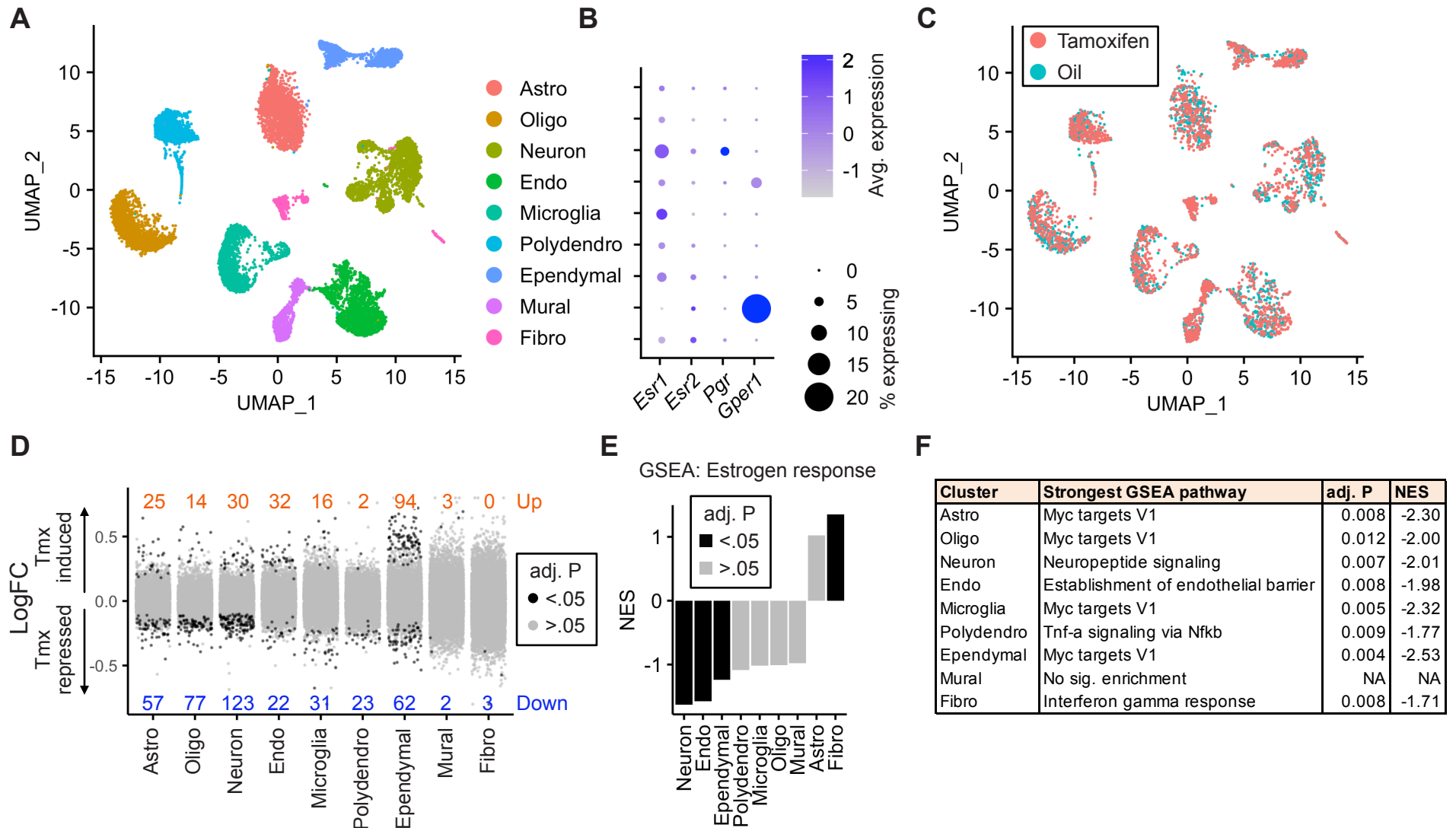148   may be modest with respect to global transcriptional signatures.

Figure 3. Tamoxifen treatment induces gene expression changes in various cell types of the hypothalamus

(**A**) UMAP showing clustering of the major cell types of the hypothalamus based on single cell transcriptomics. (**B**) Dot plot showing expression of estrogen and progesterone receptors in hypothalamic cell types. (**C**) UMAP of hypothalamic cells, comparing cells derived from female mice receiving daily tamoxifen injections (pink) or daily oil injections (blue). (**D**) Collapsed volcano plots showing differential gene expression, represented as log base 2 of fold change (LogFC), induced by daily tamoxifen treatment in various cell types of the hypothalamus. Up/Down numbers refer to total number of significantly (Bonferroni adj. P < .05) up and down regulated genes. (**E**) GSEA to find tamoxifen induced signatures of estrogen response in hypothalamic cell types. (**F**) Most strongly enriched or depleted pathways in GSEA comparing control to tamoxifen treated cells. All analyses done from cells harvested from female mice injected daily with oil (n=3) or tamoxifen (n=5) over 28 days.
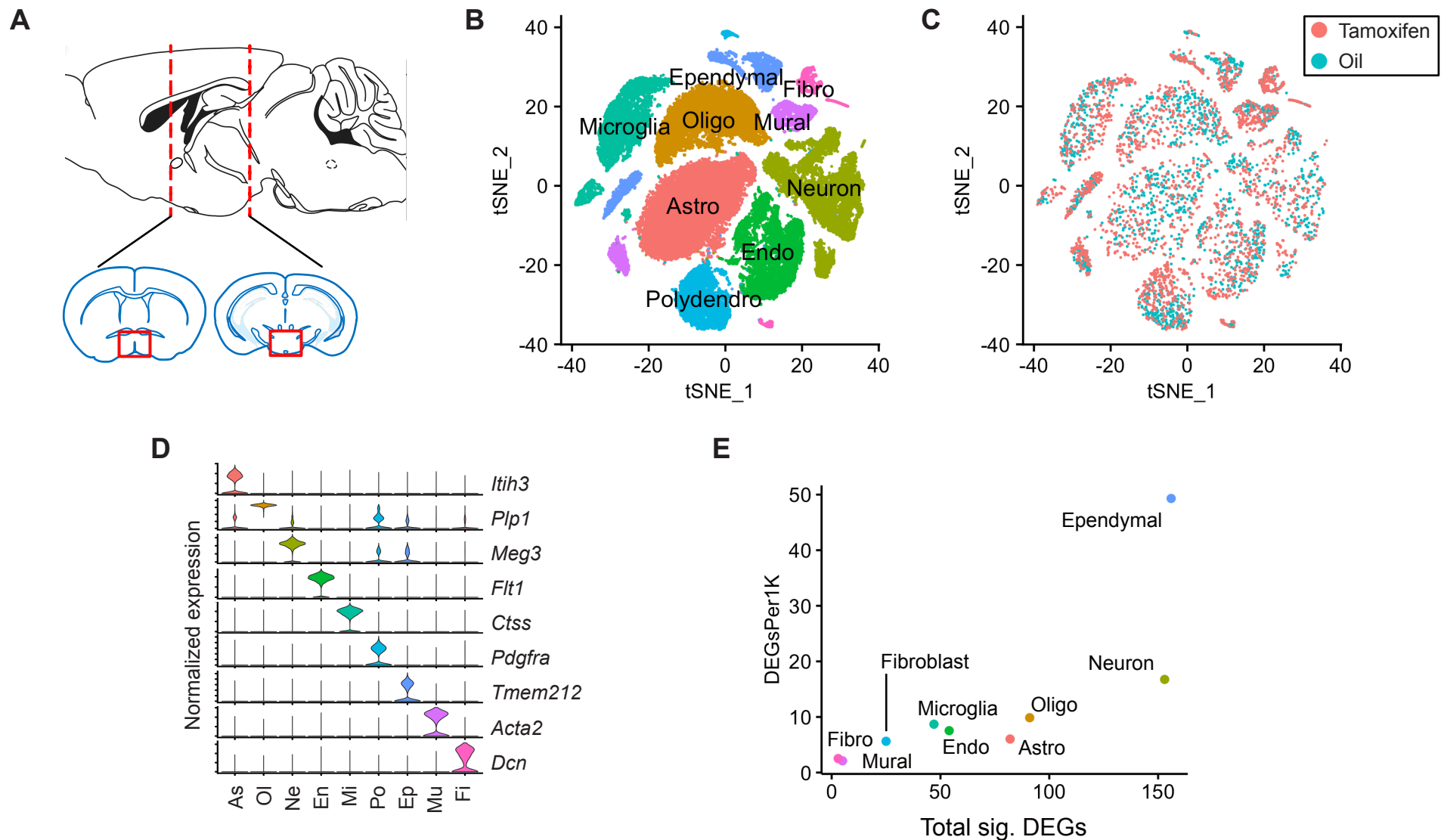
Figure 3 - Supplement 1 - Tamoxifen treatment induces gene expression changes in various cell types of the hypothalamus

(A) Schematic of the hypothalamic area dissected for scRNA-seq (Bregma +0.4 to –3 mm). (B) tSNE showing clustering of the major cell types of the hypothalamus based on single cell transcriptomics. (C) tSNE of hypothalamic cells, comparing cells derived from female mice receiving 28 daily tamoxifen injections (pink) or 28 daily oil injections (blue). (D) Violin plots showing normalized expression of cluster defining markers in all clusters. (E) Plot comparing the total number of significant (Bonferroni adj. P < .05) tamoxifen regulated genes to the number of significant tamoxifen regulated genes per thousand cells in each cluster. All analyses done from cells harvested from female mice injected daily with oil (n=3) or tamoxifen (n=5) over 28 days.

149   Amongst all cell types, neurons and ependymal cells were most sensitive to tamoxifen

150   administration, as indicated by the number of significantly induced and repressed genes (Figure

151   3D). To account for the effect of cluster size on statistical power, we also calculated the number

152   of significant differentially expressed genes per 1k cells in each cluster. Again, neurons and

153   ependymal cells have the highest numbers of differentially expressed genes when expressed as

154   total or as a fraction of the number of cells sampled (Figure 3 – Supplement 1E), suggesting the

155   strongest tamoxifen responsiveness. Although mural cells show significant enrichment of *Gper1*,

156   tamoxifen administration was associated with relatively few significant gene expression changes

157   in these cells (Figure 3D), indicating that *Gper1* does not likely mediate tamoxifen induced gene

158   expression in the hypothalamus. It is possible, however, that tamoxifen affects cellular state in a

159   non-transcriptional manner, via *Gper1*. Gene set enrichment analysis (GSEA) using a gene set

160   for estrogen response (GO:0043627) further identifies neurons and ependymal cells as markedly

161   tamoxifen responsive: tamoxifen administration induced a significant downregulation of genes

162   involved in estrogen response in neurons, endothelial cells, and ependymal cells (Figure 3E,

163   Table S1). Individual gene expression changes which may be of interest can be queried at

164   https://correalab.shinyapps.io/tamoxifenshiny/.

165   GSEA with a collection of 40 hallmark pathways and brain-focused gene ontology gene

166   sets (Table S2) revealed that all cell types except for mural cells showed significant enrichment

167   or depletion of genes in at least one pathway (Figure 3F). Significantly enriched pathways (Table

168   S3), show both overlapping and distinct effects by cell type. For example, tamoxifen treatment

169   decreased the expression of genes annotated as targets of the proto-oncogene, *Myc*, in

170   astrocytes, oligodendrocytes, neurons, endothelial cells, microglia, polydendrocytes, and

171   ependymal cells. Other cell-type specific pathways were also enriched or depleted, including:

172   establishment of the endothelial barrier in endothelial cells, neuropeptide signaling in neurons,

173   E2F targets in astrocytes, and fatty acid metabolism in ependymal cells. Together these findings

174   suggest that tamoxifen treatment has widespread effects on the hypothalamus, altering

175   transcriptional programs and cell function in both general and cell-type specific ways.

176

177   **Tamoxifen treatment causes gene expression changes in neuronal sub-types of the**

178   **hypothalamus**

179   Given the transcriptional effects of tamoxifen treatment observed in neurons and the

180   heterogeneity of estrogen-sensitive neurons within the hypothalamus, we next examined the

181   effect of tamoxifen therapy within individual neuronal clusters. Neuronal sub-clustering resulted

182   in 25 apparent hypothalamic neuronal sub-types (Figure 4A). The majority of clusters were

183   marked by expression of genes previously demonstrated to delineate hypothalamic neuronal

184   types (Figure 4B) *(Chen et al. 2017, Romanov et al. 2017, Kim et al. 2019, van Veen et al. 2020)*.

185   Markers of neuronal subtypes include neuropeptides, transcription factors, and cellular signaling

186   messengers. *Esr1* expression was observed in various neuronal subclusters (Figure 4B), but was

187   significantly enriched in neurons expressing the neuropeptide precursor, *Tac2* (log2FC = 1.08,

188   adj. P = 5.7e-98 compared to all other neuronal subclusters). GSEA demonstrates that overall,

189   tamoxifen administration is associated with a significant downregulation of genes involved in

190   neuropeptide signaling, a critical aspect of neuronal function, as well as the two principal

191   components fueling the sizeable energy demands of neuronal metabolism: oxidative

192   phosphorylation and glycolysis *(Yellen 2018)* (Figure 4C). Notably, it has previously been shown

193   that estrogens can directly regulate these metabolic pathways in the brain *(Brinton 2008, Brinton*

194   *2009)*. When divided into sub-types, few statistically significant gene expression changes caused

195   by tamoxifen were observed, likely due to loss of statistical power resulting from relatively few

196   cells in each individual cluster (Figure 4 – Supplement 1A). To gain a preliminary view at the effect

197   of tamoxifen on individual neuronal sub-types, we performed GSEA on all clusters; 14 of 25

198   neuronal types showed enrichment of at least one pathway (Table S4). Neurons marked by

199   expression of *Tac2* showed significant enrichment or depletion of the most pathways (Figure 4 –
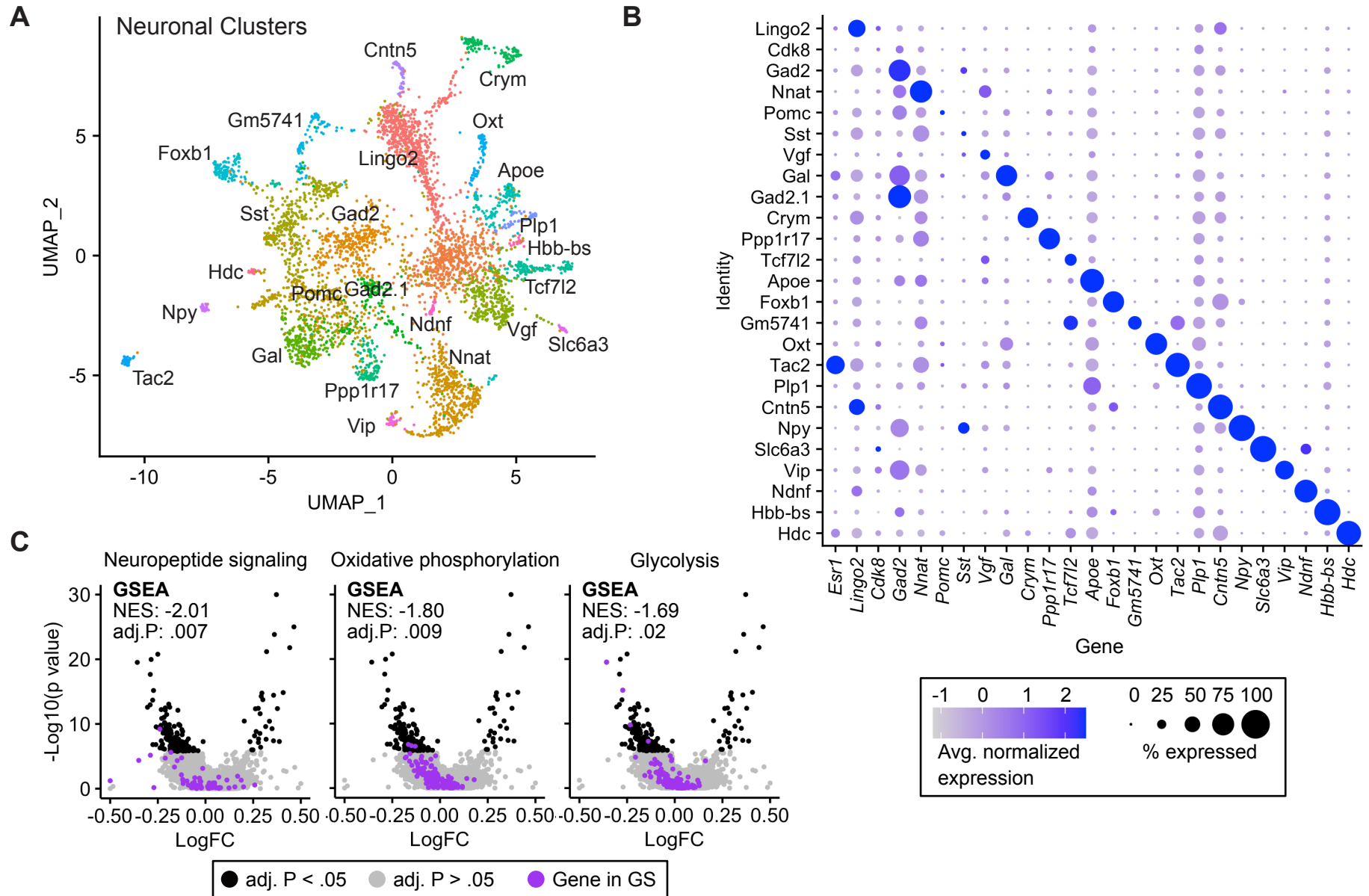
Figure 4. Tamoxifen induced gene expression changes in neurons of the hypothalamus

(**A**) UMAP showing clustering of the neuronal sub-types of the hypothalamus based on single cell transcriptomics, overlayed with identity named for top expressed cluster defining marker gene. (**B**) Dot plot showing expression of neuronal cluster defining markers and *Esr1*. (**C**) Volcano plots of tamoxifen induced or repressed DEGs overlayed with gene sets (GS) involved in neuropeptide signaling, oxidative phosphorylation, or Glycolysis. Analyses done from female mice injected daily with oil (n=3) or tamoxifen (n=5) over 28 days.
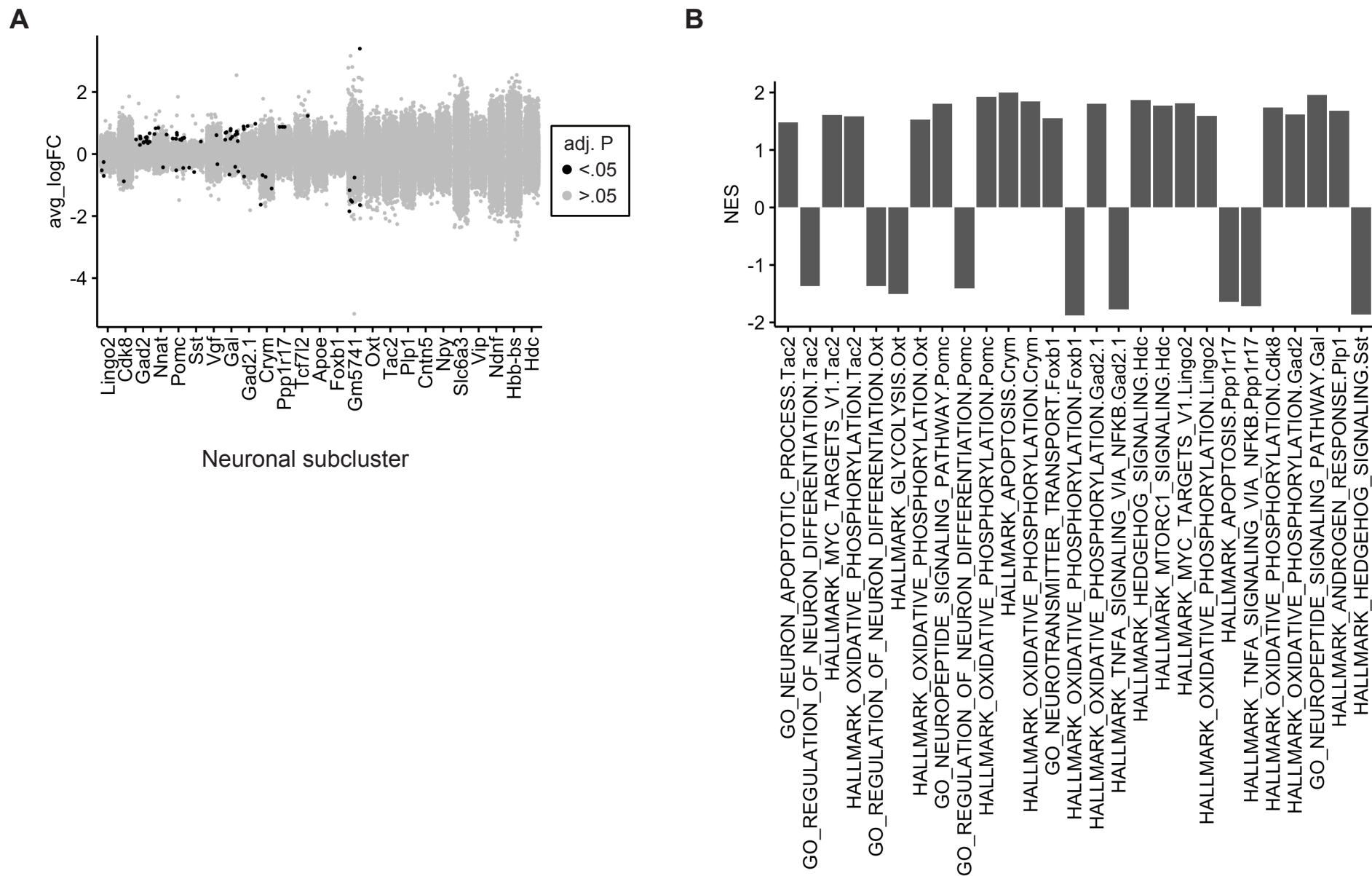
Figure 4 - Supplement 1 - Tamoxifen induced gene expression changes in neurons of the hypothalamus

(**A**) Collapsed volcano plot of differences in gene expression associated with tamoxifen treatment in the various neuronal sub-types.
(**B**) GSEA pathways significantly (adj. P < .05) upregulated or downregulated by tamoxifen in individul neuronal subclusters

200 Supplement 1B). Interestingly, examining individual pathways shows differential responses by

201 neuronal subtype. For example, genes involved in oxidative phosphorylation appear

202 downregulated by tamoxifen in neurons expressing *Foxb1*, but the same gene set is upregulated

203 in neurons expressing *Tac2* (Fig 4 – Supplement 1B). These cell-type specific effects highlight

204 the additional insights that can be revealed by scRNA-seq compared to overall averages

205 determined by bulk tissue sequencing. Additionally, these results are compatible with the previous

206 findings that tamoxifen can have different effects in different regions of the brain *(Wilson et al.*

207 *2003, Chen et al. 2014, Gibbs et al. 2014, Aquino et al. 2016, Sa et al. 2016)* and consistent with

208 cell-type-specific effects of tamoxifen within hypothalamic neurons.

209

210 **Esr1 knockout ablates hypothalamic gene expression responses to tamoxifen**

211 As *Esr1* is a known target of tamoxifen that is expressed in the hypothalamus (Figure 3B),

212 we sought to determine the impact of hypothalamic *Esr1* knockout on hypothalamic gene

213 expression responses to tamoxifen administration. The transcription factor, *Nkx2-1*, is highly

214 enriched in the medial basal hypothalamus and *Esr1^{F/F}*; *Nkx2-1^{Cre}* (*Esr1^{cKO}*) mice display a

215 selective loss of ERα immunoreactivity in the hypothalamus *(Herber et al. 2019)*. Single-cell

216 expression analysis was unable to detect a significant decrease of *Esr1* expression in any cell

217 type of *Esr1^{cKO}* mice, but clearly demonstrated that the NK2 homeobox transcription factor *Nkx2-*

218 *1* was enriched in neurons and in ependymal cells (Figure 5 – Supplement 2A). We also confirmed

219 that *Esr1^{F/F}*; *Nkx2-1^{Cre}* (*Esr1^{cKO}*) mice displayed a loss of ERα immunoreactivity in the

220 hypothalamus, including the medial preoptic area (MPA), ventrolateral subdivision of the

221 ventromedial nucleus of the hypothalamus (VMHvl), and arcuate nucleus of the hypothalamus

222 (ARC) (Figure 5A). These regions show highly enriched ERα expression *(Merchenthaler et al.*

223 *2004)* and mediate the primary hypothalamic effects of estrogens on body temperature *(Xu et al.*

224 *2011, Mauvais-Jarvis et al. 2013, Martinez de Morentin et al. 2014)*, physical activity *(Correa et*

225 *al. 2015, van Veen et al. 2020)* and bone regulation *(Farman et al. 2016, Herber et al. 2019)*.
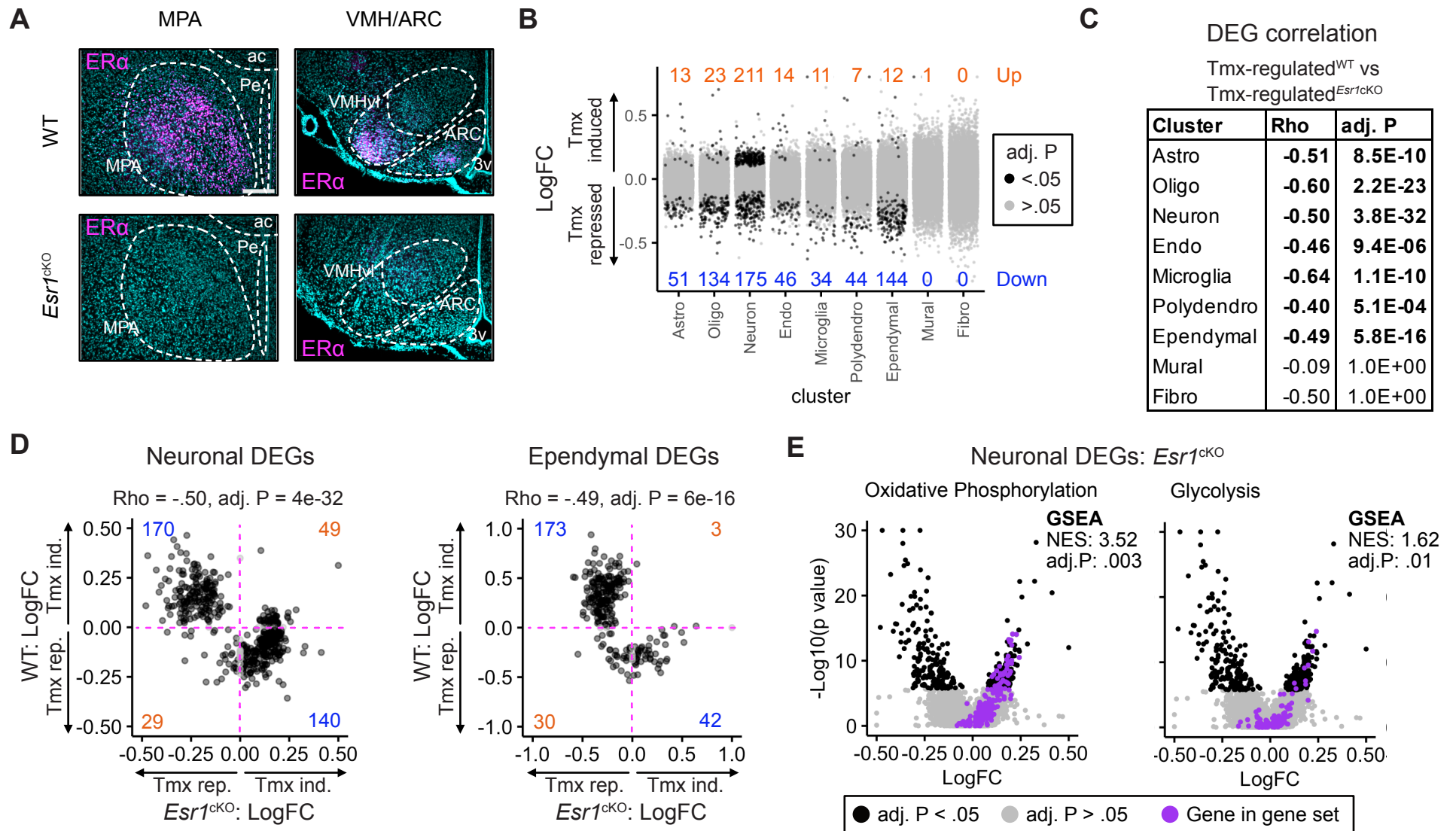
Zhang et al. Figure 5

Figure 5. *Esr1* **knockout reverses hypothalamic responses to tamoxifen**

(**A**) Immunoreactive staining of ERα in the MPA, VMH, and the ARC of ERα knockout and wild-type female mice. Scale bar: 200 um. (**B**) Differential gene expression induced by daily tamoxifen treatment in cell types of the *Esr1^f/f^;Nkx2-1^Cre^* (*Esr1^cKO^*) hypothalamus. Up/ Down numbers refer to total number of significantly (Bonferroni adj. P < .05) up and down regulated genes. (**C**) Table of correlations showing how tamoxifen induced gene expression changes in WT cells correlate with tamoxifen induced gene expression changes in *Esr1^cKO^* cells. (**D**) Gene by gene comparison of how tamoxifen treatment affects expression in wild-type and *Esr1^cKO^* neurons and ependymal cells. Blue numbers indicate ERα dependent DEGs, orange numbers indicate ERα independent DEGs (**E**) Volcano plots of all tamoxifen induced or repressed DEGs (black) overlayed with gene sets (purple) involved in oxidative phosphorylation or glycolysis. Data from n = 4 oil treated *Esr1^cKO^* and n = 4 tamoxifen treated *Esr1^cKO^*, n = 3 oil treated WT and n = 5 tamoxifen treated WT mice.

226   To test the effect of tamoxifen administration on gene expression in mice lacking

227   hypothalamic ERα, *Esr1*cKO mice received the same daily tamoxifen or vehicle injection regimen

228   concurrently with wild-type mice (Figure 1A). UMAP Clustering of all 4 treatment conditions:

229   vehicle or tamoxifen in wild-type or *Esr1*cKO animals did not reveal clear separation in global

230   transcriptional signature between any treatment group when considering all cell types (Figure 5 –

231   supplement 1A) or re-clustered neuronal sub-types (Figure 5 – Supplement 1B). *Esr1*cKO animals

232   showed proportionally fewer astrocytes and more oligodendrocytes than wild-type animals

233   (Figure 5 – Supplement 1C), though all other cell types were recovered at similar proportions.

234   Tamoxifen treatment was not associated with any significant differences in recovered cell type

235   proportions (Figure 5 – Supplement 1D).

236   Interestingly, tamoxifen treatment led to significant transcriptional changes in the

237   hypothalamus of *Esr1*cKO mice (Figure 5B). Similar to wild-type, *Esr1*cKO neurons and ependymal

238   cells were the cell-types most sensitive to tamoxifen administration compared to all other cell

239   types, as indicated by the number of significantly induced and repressed genes (Figure 5B). To

240   look closer at the specific effects of tamoxifen on gene regulation, we examined only those gene

241   expression changes that were significant in either wild-type or *Esr1*cKO cells. When comparing

242   how tamoxifen affected gene expression in wild-type mice versus how tamoxifen affected the

243   same genes in *Esr1*cKO mice, there was a strong negative Spearman correlation observed in all

244   cell types, except the poorly powered mural cells and fibroblasts (Figure 5C). This negative

245   correlation implies that the majority of significant tamoxifen-induced gene expression changes

246   that were observed in hypothalamic cell types of wild-type female mice were ablated or regulated

247   in the opposite direction in *Esr1*cKO animals.

248   In wild-type neurons, the majority of tamoxifen-regulated genes were repressed by

249   tamoxifen (Figure 3D). In *Esr1*cKO neurons, most of these genes are no longer repressed by

250   tamoxifen (Figure 5D, Key: Figure 5 – Supplement 2B). Together these data suggest that

251   tamoxifen has generally suppressive effects on neuronal transcription, and that these effects are
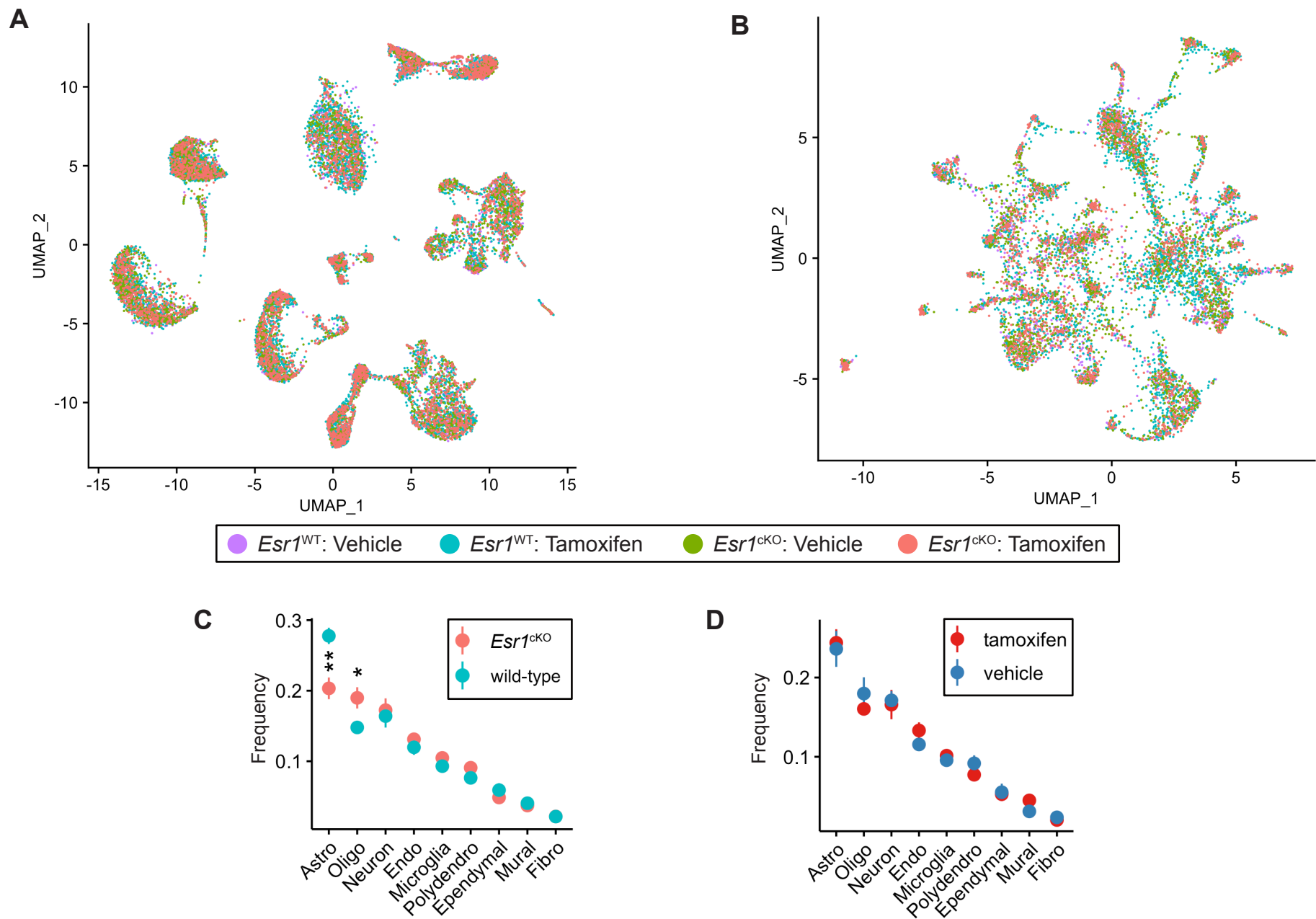
Figure 5 - Supplement 1 - identification of distinct cell clusters in 4 aligned treatment groups

(**A**) UMAP of all hypothalamic cell types showing the four studied treatment groups. (**B**) UMAP of hypothalamic neuronal types showing the four studied treatment groups. (**C,D**) Proportion of each cell type recovered, comparing *Esr1*cKO to wild-type **C** and tamoxifen to vehicle **D**. Two way anova shows effect of *Esr1* genotype on proportion of astrocytes (F = 13.3 adj. P = .003) and oligodendrocytes (F = 7.8, adj. P = .016), but no effect of tamoxifen treatment on proportion of any cell type.
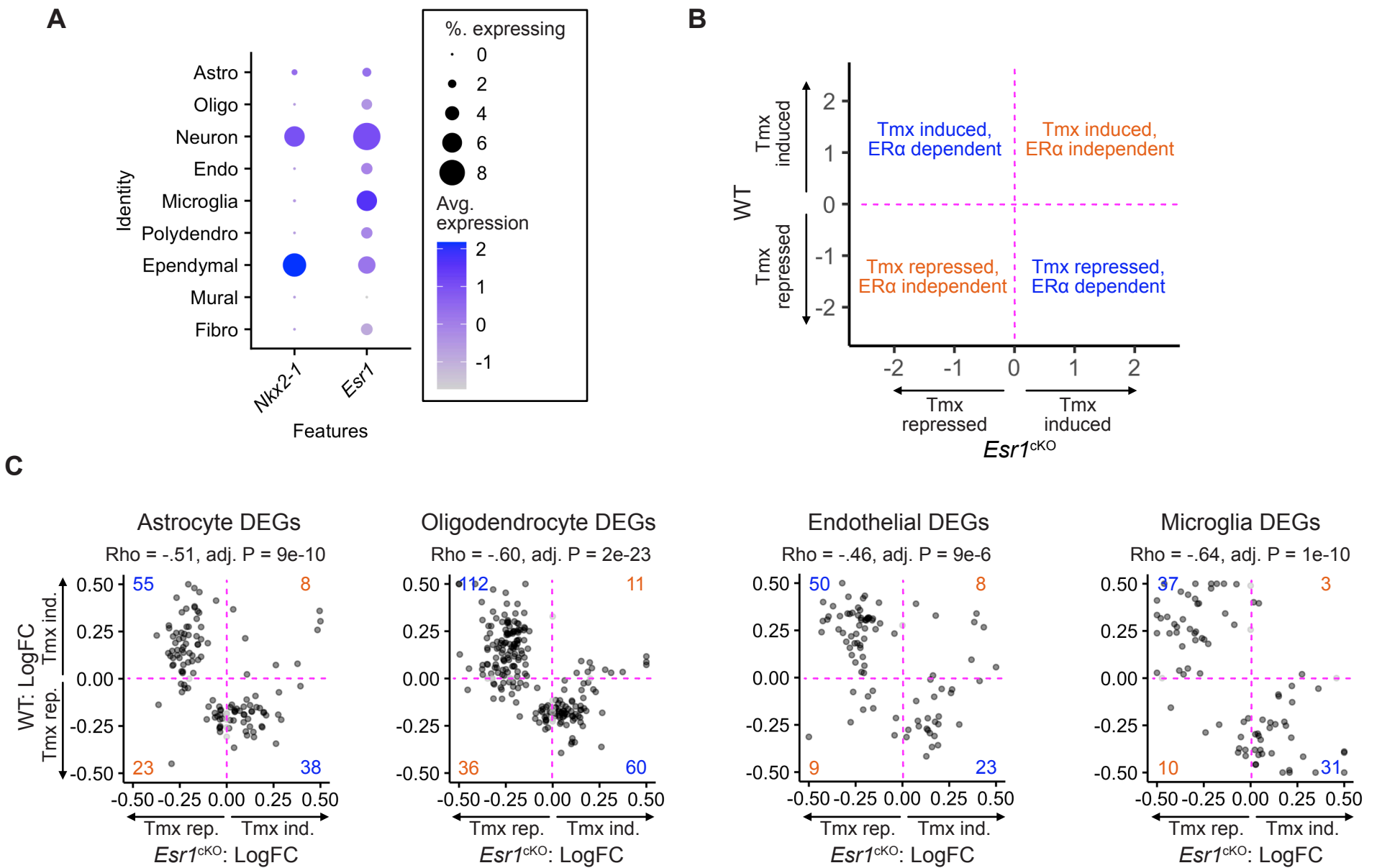
Figure 5 - Supplement 2 - Comparison of gene expression changes by tamoxifen in WT and *Esr1*[cKO] mice.

(**A**) Dotplot showing expression of *Esr1* and *Nkx2-1* in the major cell types of the hypothalamus. (**B**) Key to comparison of genes induced by tamoxifen in wild-type cells compared to how they are regulated by tamoxifen in *Esr1*[cKO] animals. (**C**) Gene by gene comparisons of how tamoxifen treatment affects expression in wild-type and *Esr1*[cKO] cells. Only genes significantly up or downregulated by tamoxifen in either wild-type or mutant cells are shown.

252   largely dependent on *Esr1*. In wild-type ependymal cells, the majority of regulated genes were

253   induced by tamoxifen (Figure 3D). Again, this induction is largely dependent on the presence of

254   ERα, as most genes induced by tamoxifen in wild-type ependymocytes were not induced by

255   tamoxifen in *Esr1*cKO ependymocytes. Despite displaying far fewer differentially expressed genes

256   in either genotype, the other cell types showed similar trends (Figure 5 – Supplement 2C).

257   To determine if the overall opposite effects of tamoxifen in *Esr1*cKO animals was associated

258   with similar changes in functional pathways, we performed GSEA with all cell type clusters as

259   before. Indeed, many pathways were altered in opposite directions in *Esr1*cKO cells compared to

260   wild-type cells following tamoxifen treatment (Complete results: Tables S2,S5). This pattern

261   included *Myc* targets in endothelial cells, ependymal cells, neurons, oligodendrocytes, and

262   polydendrocytes. Importantly, we also found a significant change of metabolic gene expression

263   in neurons, as both oxidative phosphorylation and glycolysis were upregulated by tamoxifen in

264   *Esr1*cKO neurons (Figure 5E) but downregulated in wild-type neurons (Figure 4C). This trend of

265   opposing effects of tamoxifen was not universal, as *Tnf-a* signaling was significantly

266   downregulated by tamoxifen in both *Esr1*cKO and wild-type endothelial cells. Finally, many

267   pathways, including *mTorc1* signaling in astrocytes, establishment of the endothelial barrier in

268   endothelial cells, and neuropeptide signaling in neurons, were significantly affected by tamoxifen

269   in wild-type cells, but not affected in their *Esr1*cKO counterparts.

270   GSEA for estrogen responsive genes in all cell types showed that tamoxifen

271   downregulated estrogen targets in multiple cell types of the wild-type hypothalamus but did not

272   significantly affect the same genes in cells of the *Esr1*cKO hypothalamus, even when using a

273   promiscuous cutoff or significance (Figure 5 – Supplement 3A, Table S1,S6). Similarly, GSEA in

274   individual neuronal subclusters showed that tamoxifen broadly downregulated estrogen targets in

275   wild-type neuronal subtypes, and while we still observed some downregulation of estrogen

276   responsive genes in neuronal subtypes, there was never a significant upregulation of estrogen

277   responsive genes by tamoxifen, even when using a permissive cutoff for significance (Figure 5 –

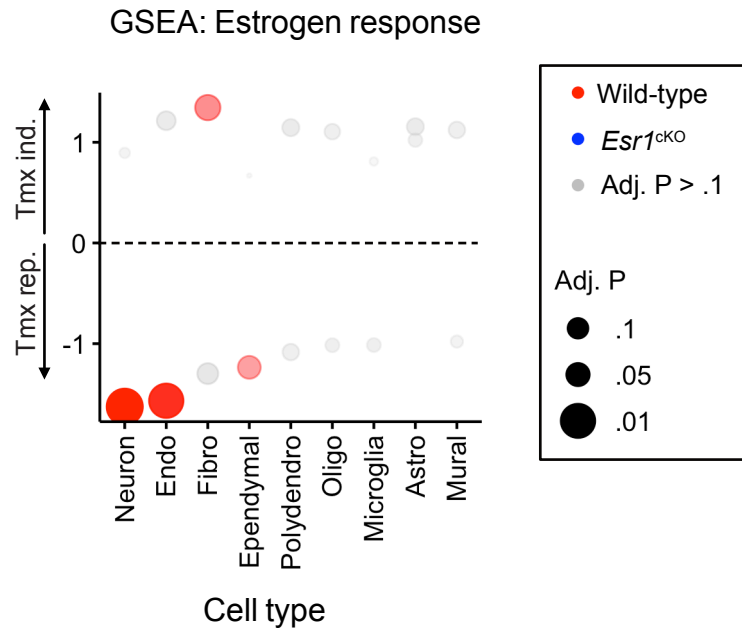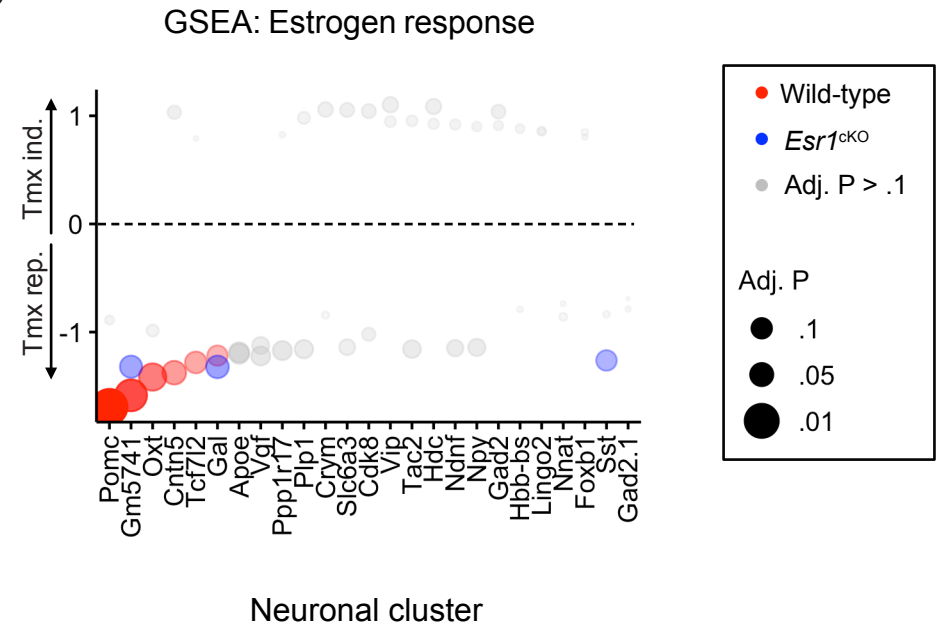**Figure 5 - Supplement 3 - Comparison of gene expression changes by tamoxifen in WT and *Esr1*cKO mice.**

(**A**) GSEA normalized enrichment scores (NES) showing tamoxifen regulation of estrogen responsive genes in wild-type and *Esr1*cKO hypothalamic cell types. (**B**) GSEA normalized enrichment scores (NES) showing tamoxifen regulation of estrogen responsive genes in wild-type and *Esr1*cKO neuronal sub-types.

278   Supplement 3B, Table S7,S8). Together these data indicate that hypothalamic expression of ERα

279   is required for a large proportion of the gene expression changes normally induced by tamoxifen,

280   including many functional pathways and those controlling neuronal activity and estrogen targets

281   in many cell types and neuronal subtypes. Individual gene expression changes which may be of

282   interest can be queried at https://correalab.shinyapps.io/tamoxifenshiny/.

283

284   **The homeostatic effects of tamoxifen are dependent on hypothalamic ERα**

285   Given the known roles of hypothalamic ERα in mediating many aspects of physiology, as

286   well as the effect of hypothalamic ERα knockout on cellular tamoxifen response, we sought to ask

287   if hypothalamic loss of ERα would also affect mouse physiological responses to tamoxifen

288   treatment. We therefore measured body temperature, physical activity and bone density in

289   *Esr1*cKO mice treated equivalently and concurrently with wild-type animals (Figure 1A).

290   Interestingly, tamoxifen injection was not associated with any difference in core body temperature

291   in *Esr1*cKO mice compared to vehicle-treated controls (Figure 6A-B). Specifically, we observed no

292   significant differences in heat dissipation or production when comparing tamoxifen to vehicle

293   treatment in *Esr1*cKO mice, as indicated by HLI (Figure 6C-D) and BAT temperature (Figure 6E-

294   F). In contrast to wild-type mice, there was no significant difference in physical activity between

295   tamoxifen and vehicle treatment in *Esr1*cKO mice (Figure 6G-H).

296   Knockout of ERα in the hypothalamus largely blocked the effect of tamoxifen on bone

297   physiology as well. No difference was observed in bone volume fraction, thickness or separation

298   of trabeculae when comparing tamoxifen to vehicle treated animals. In contrast to wild-type mice,

299   we observed a tamoxifen-induced reduction in trabecular number (Figure 6I-J). There was no

300   significant difference in bone volume ratio or cortical thickness in the cortical bones of mice treated

301   with tamoxifen compared to mice treated with vehicle (Figure 6I and K). Taken together, these

302   results suggest that the dysregulation of core temperature, reduced movement, and changed
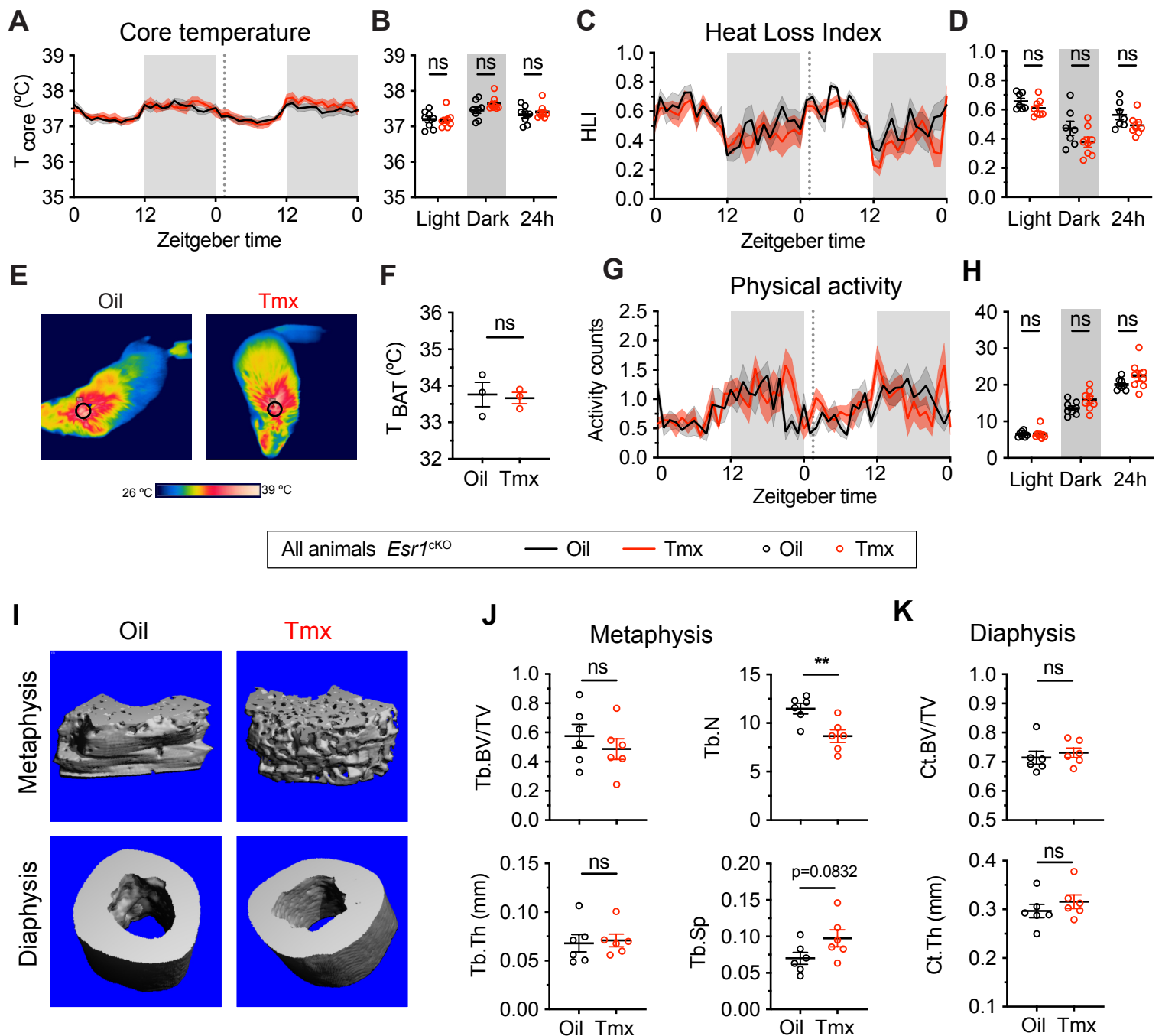
Zhang et al. Figure 6

Figure 6. The homeostatic effects of tamoxifen are dependent on hypothalamic ERα. (**A**) Hourly average of core body temperature over 2 days before and 3 weeks after injections (dotted line). (**B**) Average core body temperature from mice shown in panel **A** highlighting per animal averages in light (7:00 to 19:00), dark (19:00 to 7:00), and total 24 h periods (n=8, treatment P=0.7144). (**C**) Heat loss index (HLI) calculated from continuous measurements of core and tail temperature. (**D**) Average HLI from mice shown in panel **C** (n=7-8, P=0.1013). (**E**) Thermographic images of interscapular skin above brown adipose tissues depots in mice injected with either oil or tamoxifen. (**F**) Quantification of temperature of skin above intrascapular BAT depots (n=3, P=0.8048). (**G**) Hourly average of physical activity over 2 days before and after injections (dotted line). (**H**) Average physical activity from mice shown in panel **H** (n=8, P=0.1266). (**I**) Representative microCT images showing bone density of the distal metaphysis and midshaft diaphysis of femurs from tamoxifen or oil treated *Esr1*cKO female mice. (**J**) Trabecular bone volume fraction (BV/TV), trabecular numbers (Tb.N), trabecular thickness (Tb.Th) and trabecular separation (Tb.Sp) in distal metaphysis of femurs (n=6). (**K**) Bone volume fraction (Ct.BV/TV) and cortical thickness (Ct.Th) in diaphysis of femurs (n=6). Line shading and error bars represent SEM. ns, non-significant; **, P<0.01 for Sidak's multiple comparisons test (**B**, **D** and **H**) or two tailed t-test (**F**, **J** and **K**).

303   bone physiology associated with tamoxifen treatment in wild-type mice are largely dependent

304   upon the expression of ERα in the *Nkx2-1* lineage.

305

306   **Discussion**

307   Tamoxifen is a selective estrogen receptor modulator that exerts antiproliferative effects

308   on cancer cells through ERα *(Davies et al. 2011)*, but can exert agonistic or antagonistic effects

309   on the different estrogen receptors depending on cell type and context *(Watanabe et al. 1997, Mo*

310   *et al. 2013)*. The medial basal hypothalamus is rich in estrogen receptor expression, making it a

311   prime candidate as a tamoxifen target *(Merchenthaler et al. 2004, Gofflot et al. 2007, Matsuda et*

312   *al. 2013, Saito et al. 2016)*. Here we take the first steps to define the cell types and cellular

313   mechanisms that mediate some of the undesirable side effects experienced by people undergoing

314   tamoxifen therapy. We demonstrate the utility of mice as a good model to study many of

315   tamoxifen's physiological effects; tamoxifen administration in mice increases heat dissipation,

316   decreases movement, and increases bone density. These effects are similar to those experienced

317   by people receiving tamoxifen therapy, who experience hot flashes, lethargy, and changes in

318   bone density, amongst other symptoms *(Love et al. 1991, Powles et al. 1996, Fisher et al. 1998,*

319   *Loprinzi et al. 2000, Haghighat et al. 2003, Howell et al. 2005, Kligman et al. 2010, Francis et al.*

320   *2015)*.

321   Using single cell RNA sequencing, we find that tamoxifen alters transcriptomes in the

322   hypothalamus, consistent with the hypothesis that tamoxifen therapy alters central nervous

323   system function *(Eberling et al. 2004, Gibbs et al. 2014, Denk et al. 2015)*. Indeed, tamoxifen and

324   its metabolites are detectable and up to 46-fold higher in the brain than in serum of breast cancer

325   patients *(Lien et al. 1991)*. We report that tamoxifen treatment affects gene expression in many

326   cell types of the hypothalamus, but most strongly in neurons and ependymal cells. These findings

327   are consistent with previous reports of tamoxifen-induced gene expression changes within

328   neurons *(Lopez et al. 2006, Aquino et al. 2016, Sa et al. 2016)*, and tamoxifen-induced stress in

329   neurons and ependymal cells *(Denk et al. 2015)*. Importantly, we detect minor changes in the

330   proportion of different cell types after 28-days of treatment with a clinically relevant dose (0.1

331   mg/kg) of tamoxifen. This result is in contrast to evidence that the much higher doses used to

332   activate tamoxifen-inducible mouse models (25-100 mg/kg) can inhibit neural progenitor cell

333   proliferation during cortical patterning or induce adipogenesis and prolonged genetic effects *(Ye*

334   *et al. 2015, Lee et al. 2020)*.

335   Notably, conditional knockout of the *Esr1* gene encoding ERα did not render the brain

336   insensitive to tamoxifen. Instead it ablated or reversed the direction of a significant number of the

337   tamoxifen induced gene expression changes that were observed in the wild-type hypothalamus.

338   Importantly, this reversal encompassed many functional pathways including those controlling

339   metabolism and neuropeptide signaling in neurons. The many transcriptional changes induced

340   by tamoxifen in *Esr1*^cKO mice might be attributed to tamoxifen's effects on the other estrogen

341   receptors or effects mediated by cells outside of the *Nkx2-1* lineage. Indeed, studies of breast

342   cancer resistance suggest many other signaling pathways, e.g., progesterone receptor, androgen

343   receptor and GPER, may be involved in the actions of tamoxifen on transcription *(Mo et al. 2013,*

344   *Rondón-Lagos et al. 2016)*. Indeed, progesterone receptor expression in the hypothalamus is

345   regulated by both endogenous estrogens and tamoxifen *(Sa et al. 2016)* and we find that *Pgr* is

346   most abundant in neurons. Although more enriched in mural cells, GPER has been shown to

347   increase acetylcholine release in neurons of the hippocampus *(Gibbs et al. 2014)*. Nevertheless,

348   conditional knockout of ERα in the hypothalamus blocked the majority of the physiological

349   changes observed in wild-type mice by tamoxifen, indicating a pivotal role of ERα in mediating

350   the homeostatic effects of tamoxifen. Together, these data indicate an indispensable role of

351   hypothalamic ERα in the molecular and physiological response to tamoxifen therapy in mice. In

352   addition, our data indicate that tamoxifen exerts potent effects on gene expression in a variety of

353   neuronal subtypes, as well as in ependymal cells. It is very likely that the pleiotropic physiological

354   effects of tamoxifen involve various estrogen responsive cells and hypothalamic regions.

355   Determining which hypothalamic nuclei respond directly to tamoxifen and which nuclei mediate

356   the various effects of tamoxifen will require careful region and cell-type specific *Esr1* deletion

357   studies.

358   Hot flashes are one of the most common complaints by people undergoing tamoxifen

359   therapy or transitioning to menopause *(Stearns et al. 2002, Kligman and Younus 2010)*. Hot

360   flashes are characterized by frequent, sudden increases of heat dissipation from the skin, often

361   accompanied with sweats and transient decreases in core body temperature *(Stearns et al. 2002)*.

362   The precise mechanisms behind this change in thermoregulation are unknown, however several

363   studies have suggested that a disruption in sex hormone related central control of thermal

364   homeostasis is involved. It has been proposed that this dysregulated heat dissipation is due to a

365   lowered body temperature setpoint, which is influenced by changes in ovarian hormones including

366   estrogens and luteinizing hormone *(Dacks et al. 2010, Dacks et al. 2011, Rance et al. 2013)*. The

367   hypothalamus, a central site for both sex hormone action and body temperature regulation,

368   appears to play a key role in the etiology of hot flashes. Specifically, activating KNDy (kisspeptin,

369   neurokinin B and dynorphin expressing) neurons, which also express ERα, in the ARC increases

370   heat loss from the tail in mice *(Padilla et al. 2018)*. Conversely, ablation of KNDy neurons

371   *(Mittelman-Smith et al. 2012)* or pharmacologically blocking the Neurokinin 3 receptor (NK3R) in

372   the preoptic area (POA) *(Prague et al. 2017, Padilla et al. 2018)* was able to relieve hot flash

373   symptoms in rodents and humans. As tamoxifen readily penetrates the blood brain barrier *(Lien*

374   *et al. 1991)* and regulates estrogen-responsive neurons in the hypothalamus *(Aquino et al. 2016,*

375   *Sa et al. 2016)*, it is plausible that tamoxifen modulates these circuits in the hypothalamus to

376   induce or increase the likelihood of hot flashes. Indeed, we detected the highest *Esr1* expression

377   levels in neurons marked by expression of the neurokinin B precursor gene, *Tac2*. Furthermore,

378   *Esr1* expressing neurons in both the ARC and the MPA develop from the *Nkx2-1* lineage and

379   therefore show loss of ERα in *Esr1*[cKO] mice (Figure 5A). These data are all consistent with the

380   hypothesis that tamoxifen induces hot flashes via estrogen-sensitive neural circuits involved in

381   thermoregulation.

382   Animal studies indicate that estrogen signaling promotes movement *(Ogawa et al. 2003,*

383   *Lightfoot 2008)*, although in humans, estrogen related activity changes remain controversial (see

384   review*(Bowen et al. 2011)*). In female breast cancer patients, there is a significant association

385   between ongoing tamoxifen usage and symptoms of fatigue *(Haghighat et al. 2003)*. Our results

386   demonstrate that ERα in the hypothalamus mediates a suppressive effect of tamoxifen on

387   movement. This is consistent with the results that ERα signaling in the hypothalamus regulates

388   physical activity in mice *(Ogawa et al. 2003, Musatov et al. 2007, Xu et al. 2011, Sano et al. 2013,*

389   *Correa et al. 2015, van Veen et al. 2020)*. Specifically, activation of ERα neurons in the *Nkx2-1*

390   lineage promotes movement *(Correa et al. 2015)* and loss of ERα in the VMH reduces physical

391   activity in mice *(Musatov et al. 2007, Correa et al. 2015)*. In addition, the POA is rich in ERα

392   expression and has been shown to be responsible for estrogen induced running wheel activity

393   *(King 1979, Fahrbach et al. 1985, Takeo et al. 1995)*. Therefore, tamoxifen may act as an ERα

394   antagonist in those estrogen-sensitive hypothalamic regions to suppress physical activity in mice.

395   Similar to endogenous estrogens, tamoxifen has profound impacts on bone remodeling.

396   Human studies have demonstrated that tamoxifen is protective against bone mineral density loss

397   in after menopause, but induces bone loss before menopause *(Love et al. 1992, Kristensen et al.*

398   *1994, Powles et al. 1996, Vehmanen et al. 2006)*. Contrasting this, animal studies have generally

399   shown protective effects of tamoxifen on bone regardless of ovarian function *(Turner et al. 1988,*

400   *Perry et al. 2005, Starnes et al. 2007)*. Whether these discrepancies are due to fundamental

401   differences between rodent and human bone biology remains to be determined. We found that

402   tamoxifen greatly increased bone mass in wild-type mice, displaying an estrogen-like protective

403   effect. Although this study did not evaluate bone formation and resorption respectively, a number

404   of animal studies have indicated that tamoxifen can stimulate bone formation *(Perry et al. 2005)*

405   and also suppress bone resorption *(Turner et al. 1988, Quaedackers et al. 2001)*, resulting in a

406   net bone accruement. Although different estrogen receptor subtypes may exert distinct effects on

407   bone regulation *(Windahl et al. 2002)*, the action of tamoxifen on bone is likely mediated by ERα

408   but not ERβ *(Quaedackers et al. 2001)*. Within the hypothalamus, depletion of ERα in the medial

409   basal hypothalamus or specifically within the KNDy neurons results in impressive increases in

410   bone mass *(Farman et al. 2016, Herber et al. 2019)*. Thus it is possible that any effects of

411   tamoxifen on bone that are masked by the already altered bone metabolism in *Esr1*cKO mice.

412   Nevertheless, we observed no effect of tamoxifen on bone volume in *Esr1*cKO mice, implying that

413   tamoxifen's effects on bone are at least partially mediated by ERα expression within the *Nkx2-1*

414   lineage.

415   Although the *Nkx2-1* lineage includes cells in the thyroid, pituitary and lung, *Esr1*

416   expression is not altered in these peripheral tissues of *Esr1*cKO mice *(Herber et al. 2019)*, leaving

417   the hypothalamus as the most likely mediator of the ERα-dependent physiological effects of

418   tamoxifen reported here. Despite this, it is very likely that peripheral tissues are also affected by

419   systemic tamoxifen administration, leading to other physiological effects that we did not examine.

420   Indeed, there is evidence that estrogen suppression therapies, including tamoxifen or aromatase

421   inhibitors, can lead to the dysregulation of energy balance and glucose homeostasis in humans

422   and when modeled in rodents *(Lopez et al. 2006, Lampert et al. 2013, Ceasrine et al. 2019, Scalzo*

423   *et al. 2020)*. Together, these studies reveal widespread effects of tamoxifen therapy on the

424   hypothalamus and implicate ERα signaling within the *Nkx2-1* lineage as a major mediator of the

425   effects of tamoxifen on thermoregulation, physical activity, and bone homeostasis.

426   In summary, the rodent model of tamoxifen therapy provided here mimics several of the

427   key side effects of endocrine therapy observed in humans and highlights a central mechanism for

428   understanding these specific adverse outcomes. A recent survey conducted in the online breast

429   cancer communities showed that women often experienced more of tamoxifen's side effects than

430   men and one-third of patients did not feel that their side effects were taken seriously *(Berkowitz*

431   *et al. 2020)*. Our study highlights many ways in which tamoxifen treatment could impact quality of

432   life in breast cancer patients and takes the first step towards understanding the mechanisms of

433   these side effects in order to develop better treatments.

434

435   **Acknowledgements**

443

444   **References**

445   Aquino, N. S., R. Araujo-Lopes, I. A. Batista, P. C. Henriques, M. O. Poletini, C. R. Franci, A. M. Reis and R.
446   E. Szawka (2016). "Hypothalamic Effects of Tamoxifen on Oestrogen Regulation of Luteinising
447   Hormone and Prolactin Secretion in Female Rats." J Neuroendocrinol **28**(1).
448   Berkowitz, M. J., C. K. Thompson, L. T. Zibecchi, M. K. Lee, E. Streja, J. S. Berkowitz, C. M. Wenziger, J. L.
449   Baker, M. L. DiNome and D. J. Attai (2020). "How patients experience endocrine therapy for breast
450   cancer: an online survey of side effects, adherence, and medical team support." Journal of Cancer
451   Survivorship: 1-11.
452   Blondel, V. D., J.-L. Guillaume, R. Lambiotte and E. Lefebvre (2008). "Fast unfolding of communities in
453   large networks." Journal of Statistical Mechanics: Theory and Experiment **2008**(10): P10008.
454   Bowe, J., X. F. Li, J. Kinsey-Jones, A. Heyerick, S. Brain, S. Milligan and K. O'Byrne (2006). "The hop
455   phytoestrogen, 8-prenylnaringenin, reverses the ovariectomy-induced rise in skin temperature in an
456   animal model of menopausal hot flushes." J Endocrinol **191**(2): 399-405.
457   Bowen, R. S., M. J. Turner and J. T. Lightfoot (2011). "Sex hormone effects on physical activity levels: why
458   doesn't Jane run as much as Dick?" Sports Med **41**(1): 73-86.
459   Brinton, R. D. (2008). "The healthy cell bias of estrogen action: mitochondrial bioenergetics and
460   neurological implications." Trends Neurosci **31**(10): 529-537.
461   Brinton, R. D. (2009). "Estrogen-induced plasticity from cells to circuits: predictions for cognitive
462   function." Trends Pharmacol Sci **30**(4): 212-222.
463   Cannon, B. and J. Nedergaard (2004). "Brown adipose tissue: function and physiological significance."
464   Physiol Rev **84**(1): 277-359.

465   Ceasrine, A. M., N. Ruiz-Otero, E. E. Lin, D. N. Lumelsky, E. D. Boehm and R. Kuruvilla (2019). "Tamoxifen
466   Improves Glucose Tolerance in a Delivery-, Sex-, and Strain-Dependent Manner in Mice."
467   Endocrinology **160**(4): 782-790.

468   Chen, R., X. Wu, L. Jiang and Y. Zhang (2017). "Single-Cell RNA-Seq Reveals Hypothalamic Cell Diversity."
469   Cell Rep **18**(13): 3227-3241.

470   Chen, X., J. Li, J. Chen, D. Li, R. Ye, J. Zhang, C. Zhu, Y. Tian and K. Wang (2014). "Decision-making
471   impairments in breast cancer patients treated with tamoxifen." Hormones and Behavior **66**(2): 449-
472   456.

473   Chlebowski, R. T., J. Kim and R. Haque (2014). "Adherence to endocrine therapy in breast cancer
474   adjuvant and prevention settings." Cancer Prev Res (Phila) **7**(4): 378-387.

475   Correa, S. M., D. W. Newstrom, J. P. Warne, P. Flandin, C. C. Cheung, A. T. Lin-Moore, A. A. Pierce, A. W.
476   Xu, J. L. Rubenstein and H. A. Ingraham (2015). "An estrogen-responsive module in the ventromedial
477   hypothalamus selectively drives sex-specific activity in females." Cell Rep **10**(1): 62-74.

478   Cuzick, J., J. F. Forbes, I. Sestak, S. Cawthorn, H. Hamed, K. Holli and A. Howell (2007). "Long-term results
479   of tamoxifen prophylaxis for breast cancer--96-month follow-up of the randomized IBIS-I trial." J Natl
480   Cancer Inst **99**(4): 272-282.

481   Dacks, P. A., S. J. Krajewski and N. E. Rance (2011). "Ambient temperature and 17beta-estradiol modify
482   Fos immunoreactivity in the median preoptic nucleus, a putative regulator of skin vasomotion."
483   Endocrinology **152**(7): 2750-2759.

484   Dacks, P. A. and N. E. Rance (2010). "Effects of estradiol on the thermoneutral zone and core
485   temperature in ovariectomized rats." Endocrinology **151**(3): 1187-1193.

486   Davies, C., J. Godwin, R. Gray, M. Clarke, D. Cutter, S. Darby, P. McGale, H. C. Pan, C. Taylor, Y. C. Wang,
487   M. Dowsett, J. Ingle and R. Peto (2011). "Relevance of breast cancer hormone receptors and other
488   factors to the efficacy of adjuvant tamoxifen: patient-level meta-analysis of randomised trials."
489   Lancet **378**(9793): 771-784.

490   Davies, C., H. Pan, J. Godwin, R. Gray, R. Arriagada, V. Raina, M. Abraham, V. H. Medeiros Alencar, A.
491   Badran, X. Bonfill, J. Bradbury, M. Clarke, R. Collins, S. R. Davis, A. Delmestri, J. F. Forbes, P. Haddad,
492   M. F. Hou, M. Inbar, H. Khaled, J. Kielanowska, W. H. Kwan, B. S. Mathew, I. Mittra, B. Muller, A.
493   Nicolucci, O. Peralta, F. Pernas, L. Petruzelka, T. Pienkowski, R. Radhika, B. Rajan, M. T. Rubach, S.
494   Tort, G. Urrutia, M. Valentini, Y. Wang, R. Peto and G. Adjuvant Tamoxifen: Longer Against Shorter
495   Collaborative (2013). "Long-term effects of continuing adjuvant tamoxifen to 10 years versus
496   stopping at 5 years after diagnosis of oestrogen receptor-positive breast cancer: ATLAS, a
497   randomised trial." Lancet **381**(9869): 805-816.

498   de Médina, P., G. Favre and M. Poirot (2004). "Multiple targeting by the antitumor drug tamoxifen: a
499   structure-activity study." Curr Med Chem Anticancer Agents **4**(6): 491-508.

500   Denk, F., L. M. Ramer, E. L. Erskine, M. A. Nassar, Y. Bogdanov, M. Signore, J. N. Wood, S. B. McMahon
501   and M. S. Ramer (2015). "Tamoxifen induces cellular stress in the nervous system by inhibiting
502   cholesterol synthesis." Acta Neuropathol Commun **3**: 74.

503   Eberling, J. L., C. Wu, R. Tong-Turnbeaugh and W. J. Jagust (2004). "Estrogen- and tamoxifen-associated
504   effects on brain structure and function." Neuroimage **21**(1): 364-371.

505   Fahrbach, S. E., R. L. Meisel and D. W. Pfaff (1985). "Preoptic implants of estradiol increase wheel
506   running but not the open field activity of female rats." Physiol Behav **35**(6): 985-992.

507   Farman, H. H., S. H. Windahl, L. Westberg, H. Isaksson, E. Egecioglu, E. Schele, H. Ryberg, J. O. Jansson, J.
508   Tuukkanen, A. Koskela, S. K. Xie, L. Hahner, J. Zehr, D. J. Clegg, M. K. Lagerquist and C. Ohlsson (2016).
509   "Female Mice Lacking Estrogen Receptor-alpha in Hypothalamic Proopiomelanocortin (POMC)

Neurons Display Enhanced Estrogenic Response on Cortical Bone Mass." Endocrinology **157**(8): 3242-3252.

Fisher, B., J. P. Costantino, D. L. Wickerham, C. K. Redmond, M. Kavanah, W. M. Cronin, V. Vogel, A. Robidoux, N. Dimitrov, J. Atkins, M. Daly, S. Wieand, E. Tan-Chiu, L. Ford and N. Wolmark (1998). "Tamoxifen for prevention of breast cancer: report of the National Surgical Adjuvant Breast and Bowel Project P-1 Study." J Natl Cancer Inst **90**(18): 1371-1388.

Francis, P. A., M. M. Regan, G. F. Fleming, I. Lang, E. Ciruelos, M. Bellet, H. R. Bonnefoi, M. A. Climent, G. A. Da Prada, H. J. Burstein, S. Martino, N. E. Davidson, C. E. Geyer, Jr., B. A. Walley, R. Coleman, P. Kerbrat, S. Buchholz, J. N. Ingle, E. P. Winer, M. Rabaglio-Poretti, R. Maibach, B. Ruepp, A. Giobbie-Hurder, K. N. Price, M. Colleoni, G. Viale, A. S. Coates, A. Goldhirsch, R. D. Gelber, S. Investigators and G. International Breast Cancer Study (2015). "Adjuvant ovarian suppression in premenopausal breast cancer." N Engl J Med **372**(5): 436-446.

Friese, C. R., T. M. Pini, Y. Li, P. H. Abrahamse, J. J. Graff, A. S. Hamilton, R. Jagsi, N. K. Janz, S. T. Hawley, S. J. Katz and J. J. Griggs (2013). "Adjuvant endocrine therapy initiation and persistence in a diverse sample of patients with breast cancer." Breast Cancer Res Treat **138**(3): 931-939.

Gibbs, R. B., D. Nelson and R. Hammond (2014). "Role of GPR30 in mediating estradiol effects on acetylcholine release in the hippocampus." Hormones and Behavior **66**(2): 339-345.

Gierach, G. L., R. E. Curtis, R. M. Pfeiffer, M. Mullooly, E. A. Ntowe, R. N. Hoover, S. J. Nyante, H. S. Feigelson, A. G. Glass and A. Berrington de Gonzalez (2017). "Association of Adjuvant Tamoxifen and Aromatase Inhibitor Therapy With Contralateral Breast Cancer Risk Among US Women With Breast Cancer in a General Community Setting." JAMA Oncol **3**(2): 186-193.

Gofflot, F., N. Chartoire, L. Vasseur, S. Heikkinen, D. Dembele, J. Le Merrer and J. Auwerx (2007). "Systematic gene expression mapping clusters nuclear receptors according to their function in the brain." Cell **131**(2): 405-418.

Gordon, C. J. (1993). Temperature Regulation in Laboratory Rodents. Cambridge, Cambridge University Press.

Haghighat, S., M. E. Akbari, K. Holakouei, A. Rahimi and A. Montazeri (2003). "Factors predicting fatigue in breast cancer patients." Support Care Cancer **11**(8): 533-538.

Herber, C. B., W. C. Krause, L. Wang, J. R. Bayrer, A. Li, M. Schmitz, A. Fields, B. Ford, Z. Zhang, M. S. Reid, D. K. Nomura, R. A. Nissenson, S. M. Correa and H. A. Ingraham (2019). "Estrogen signaling in arcuate Kiss1 neurons suppresses a sex-dependent female circuit promoting dense strong bones." Nat Commun **10**(1): 163.

Howell, A., J. Cuzick, M. Baum, A. Buzdar, M. Dowsett, J. F. Forbes, G. Hoctin-Boes, J. Houghton, G. Y. Locker, J. S. Tobias and A. T. Group (2005). "Results of the ATAC (Arimidex, Tamoxifen, Alone or in Combination) trial after completion of 5 years' adjuvant treatment for breast cancer." Lancet **365**(9453): 60-62.

Isensee, J., L. Meoli, V. Zazzu, C. Nabzdyk, H. Witt, D. Soewarto, K. Effertz, H. Fuchs, V. Gailus-Durner, D. Busch, T. Adler, M. H. de Angelis, M. Irgang, C. Otto and P. R. Noppinger (2009). "Expression pattern of G protein-coupled receptor 30 in LacZ reporter mice." Endocrinology **150**(4): 1722-1730.

Jordan, V. C. (2003). "Tamoxifen: a most unlikely pioneering medicine." Nature Reviews Drug Discovery **2**(3): 205-213.

Jordan, V. C. (2007). "New insights into the metabolism of tamoxifen and its role in the treatment and prevention of breast cancer." Steroids **72**(13): 829-842.

Kim, D. W., Z. Yao, L. T. Graybuck, T. K. Kim, T. N. Nguyen, K. A. Smith, O. Fong, L. Yi, N. Koulena, N. Pierson, S. Shah, L. Lo, A. H. Pool, Y. Oka, L. Pachter, L. Cai, B. Tasic, H. Zeng and D. J. Anderson

(2019). "Multimodal Analysis of Cell Types in a Hypothalamic Node Controlling Social Behavior." Cell **179**(3): 713-728 e717.

King, J. M. (1979). "Effects of lesions of the amygdala, preoptic area, and hypothalamus on estradiol-induced activity in the female rat." J Comp Physiol Psychol **93**(2): 360-367.

Kligman, L. and J. Younus (2010). "Management of hot flashes in women with breast cancer." Curr Oncol **17**(1): 81-86.

Krajewski-Hall, S. J., E. M. Blackmore, J. R. McMinn and N. E. Rance (2018). "Estradiol alters body temperature regulation in the female mouse." Temperature **5**(1): 56-69.

Kristensen, B., B. Ejlertsen, P. Dalgaard, L. Larsen, S. N. Holmegaard, I. Transbol and H. T. Mouridsen (1994). "Tamoxifen and bone metabolism in postmenopausal low-risk breast cancer patients: a randomized study." J Clin Oncol **12**(5): 992-997.

Lampert, C., D. M. Arcego, D. P. Laureano, L. A. Diehl, I. F. da Costa Lima, R. Krolow, L. F. Pettenuzzo, C. Dalmaz and D. Vendite (2013). "Effect of chronic administration of tamoxifen and/or estradiol on feeding behavior, palatable food and metabolic parameters in ovariectomized rats." Physiol Behav **119**: 17-24.

Lee, C.-M., L. Zhou, J. Liu, J. Shi, Y. Geng, M. Liu, J. Wang, X. Su, N. Barad, J. Wang, Y. E. Sun and Q. Lin (2020). "Single-cell RNA-seq analysis revealed long-lasting adverse effects of tamoxifen on neurogenesis in prenatal and adult brains." Proceedings of the National Academy of Sciences **117**(32): 19578-19589.

Lien, E. A., K. Wester, P. E. Lønning, E. Solheim and P. M. Ueland (1991). "Distribution of tamoxifen and metabolites into brain tissue and brain metastases in breast cancer patients." British Journal of Cancer **63**(4): 641-645.

Lightfoot, J. T. (2008). "Sex hormones' regulation of rodent physical activity: a review." Int J Biol Sci **4**(3): 126-132.

Liu, W., S. Venugopal, S. Majid, I. S. Ahn, G. Diamante, J. Hong, X. Yang and S. H. Chandler (2020). "Single-cell RNA-seq analysis of the brainstem of mutant SOD1 mice reveals perturbed cell types and pathways of amyotrophic lateral sclerosis." Neurobiology of Disease **141**: 104877.

Lopez, M., C. J. Lelliott, S. Tovar, W. Kimber, R. Gallego, S. Virtue, M. Blount, M. J. Vazquez, N. Finer, T. J. Powles, S. O'Rahilly, A. K. Saha, C. Dieguez and A. J. Vidal-Puig (2006). "Tamoxifen-induced anorexia is associated with fatty acid synthase inhibition in the ventromedial nucleus of the hypothalamus and accumulation of malonyl-CoA." Diabetes **55**(5): 1327-1336.

Loprinzi, C. L., K. M. Zahasky, J. A. Sloan, P. J. Novotny and S. K. Quella (2000). "Tamoxifen-induced hot flashes." Clin Breast Cancer **1**(1): 52-56.

Love, R. R., L. Cameron, B. L. Connell and H. Leventhal (1991). "Symptoms associated with tamoxifen treatment in postmenopausal women." Arch Intern Med **151**(9): 1842-1847.

Love, R. R., R. B. Mazess, H. S. Barden, S. Epstein, P. A. Newcomb, V. C. Jordan, P. P. Carbone and D. L. DeMets (1992). "Effects of Tamoxifen on Bone Mineral Density in Postmenopausal Women with Breast Cancer." New England Journal of Medicine **326**(13): 852-856.

Macosko, E. Z., A. Basu, R. Satija, J. Nemesh, K. Shekhar, M. Goldman, I. Tirosh, A. R. Bialas, N. Kamitaki, E. M. Martersteck, J. J. Trombetta, D. A. Weitz, J. R. Sanes, A. K. Shalek, A. Regev and S. A. McCarroll (2015). "Highly Parallel Genome-wide Expression Profiling of Individual Cells Using Nanoliter Droplets." Cell **161**(5): 1202-1214.

Martinez de Morentin, P. B., I. Gonzalez-Garcia, L. Martins, R. Lage, D. Fernandez-Mallo, N. Martinez-Sanchez, F. Ruiz-Pino, J. Liu, D. A. Morgan, L. Pinilla, R. Gallego, A. K. Saha, A. Kalsbeek, E. Fliers, P. H.

Bisschop, C. Dieguez, R. Nogueiras, K. Rahmouni, M. Tena-Sempere and M. Lopez (2014). "Estradiol regulates brown adipose tissue thermogenesis via hypothalamic AMPK." Cell Metab **20**(1): 41-53.

Matsuda, K. I., M. Yanagisawa, K. Sano, I. Ochiai, S. Musatov, K. Okoshi, S. Tsukahara, S. Ogawa and M. Kawata (2013). "Visualisation and characterisation of oestrogen receptor alpha-positive neurons expressing green fluorescent protein under the control of the oestrogen receptor alpha promoter." Eur J Neurosci **38**(2): 2242-2249.

Mauvais-Jarvis, F., D. J. Clegg and A. L. Hevener (2013). "The role of estrogens in control of energy balance and glucose homeostasis." Endocr Rev **34**(3): 309-338.

Merchenthaler, I., M. V. Lane, S. Numan and T. L. Dellovade (2004). "Distribution of estrogen receptor alpha and beta in the mouse central nervous system: in vivo autoradiographic and immunocytochemical analyses." J Comp Neurol **473**(2): 270-291.

Mittelman-Smith, M. A., H. Williams, S. J. Krajewski-Hall, N. T. McMullen and N. E. Rance (2012). "Role for kisspeptin/neurokinin B/dynorphin (KNDy) neurons in cutaneous vasodilatation and the estrogen modulation of body temperature." Proc Natl Acad Sci U S A **109**(48): 19846-19851.

Mo, Z., M. Liu, F. Yang, H. Luo, Z. Li, G. Tu and G. Yang (2013). "GPR30 as an initiator of tamoxifen resistance in hormone-dependent breast cancer." Breast Cancer Res **15**(6): R114.

Moffitt, J. R., D. Bambah-Mukku, S. W. Eichhorn, E. Vaughn, K. Shekhar, J. D. Perez, N. D. Rubinstein, J. Hao, A. Regev, C. Dulac and X. Zhuang (2018). "Molecular, spatial, and functional single-cell profiling of the hypothalamic preoptic region." Science **362**(6416).

Musatov, S., W. Chen, D. W. Pfaff, C. V. Mobbs, X. J. Yang, D. J. Clegg, M. G. Kaplitt and S. Ogawa (2007). "Silencing of estrogen receptor alpha in the ventromedial nucleus of hypothalamus leads to metabolic syndrome." Proc Natl Acad Sci U S A **104**(7): 2501-2506.

Ogawa, S., J. Chan, J. A. Gustafsson, K. S. Korach and D. W. Pfaff (2003). "Estrogen increases locomotor activity in mice through estrogen receptor alpha: specificity for the type of activity." Endocrinology **144**(1): 230-239.

Padilla, S. L., C. W. Johnson, F. D. Barker, M. A. Patterson and R. D. Palmiter (2018). "A Neural Circuit Underlying the Generation of Hot Flushes." Cell Rep **24**(2): 271-277.

Patisaul, H. B., E. A. Aultman, I. F. Bielsky, L. J. Young and M. E. Wilson (2003). "Immediate and residual effects of tamoxifen and ethynylestradiol in the female rat hypothalamus." Brain Res **978**(1-2): 185-193.

Perry, M. J., S. Gujra, T. Whitworth and J. H. Tobias (2005). "Tamoxifen stimulates cancellous bone formation in long bones of female mice." Endocrinology **146**(3): 1060-1065.

Powles, T. J., T. Hickish, J. A. Kanis, A. Tidy and S. Ashley (1996). "Effect of tamoxifen on bone mineral density measured by dual-energy x-ray absorptiometry in healthy premenopausal and postmenopausal women." J Clin Oncol **14**(1): 78-84.

Prague, J. K., R. E. Roberts, A. N. Comninos, S. Clarke, C. N. Jayasena, Z. Nash, C. Doyle, D. A. Papadopoulou, S. R. Bloom, P. Mohideen, N. Panay, M. S. Hunter, J. D. Veldhuis, L. C. Webber, L. Huson and W. S. Dhillo (2017). "Neurokinin 3 receptor antagonism as a novel treatment for menopausal hot flushes: a phase 2, randomised, double-blind, placebo-controlled trial." Lancet **389**(10081): 1809-1820.

Quaedackers, M. E., C. E. Van Den Brink, S. Wissink, R. H. Schreurs, J. A. Gustafsson, P. T. Van Der Saag and B. B. Van Der Burg (2001). "4-hydroxytamoxifen trans-represses nuclear factor-kappa B activity in human osteoblastic U2-OS cells through estrogen receptor (ER)alpha, and not through ER beta." Endocrinology **142**(3): 1156-1166.

Rance, N. E., P. A. Dacks, M. A. Mittelman-Smith, A. A. Romanovsky and S. J. Krajewski-Hall (2013). "Modulation of body temperature and LH secretion by hypothalamic KNDy (kisspeptin, neurokinin B and dynorphin) neurons: a novel hypothesis on the mechanism of hot flushes." Front Neuroendocrinol **34**(3): 211-227.

Revankar, C. M., D. F. Cimino, L. A. Sklar, J. B. Arterburn and E. R. Prossnitz (2005). "A transmembrane intracellular estrogen receptor mediates rapid cell signaling." Science **307**(5715): 1625-1630.

Romanov, R. A., A. Zeisel, J. Bakker, F. Girach, A. Hellysaz, R. Tomer, A. Alpár, J. Mulder, F. Clotman, E. Keimpema, B. Hsueh, A. K. Crow, H. Martens, C. Schwindling, D. Calvigioni, J. S. Bains, Z. Máté, G. Szabó, Y. Yanagawa, M. D. Zhang, A. Rendeiro, M. Farlik, M. Uhlén, P. Wulff, C. Bock, C. Broberger, K. Deisseroth, T. Hökfelt, S. Linnarsson, T. L. Horvath and T. Harkany (2017). "Molecular interrogation of hypothalamic organization reveals distinct dopamine neuronal subtypes." Nat Neurosci **20**(2): 176-188.

Romanovsky, A. A., A. I. Ivanov and Y. P. Shimansky (2002). "Selected contribution: ambient temperature for experiments in rats: a new method for determining the zone of thermal neutrality." J Appl Physiol (1985) **92**(6): 2667-2679.

Rondón-Lagos, M., V. E. Villegas, N. Rangel, M. C. Sánchez and P. G. Zaphiropoulos (2016). "Tamoxifen Resistance: Emerging Molecular Targets." Int J Mol Sci **17**(8).

Sa, S. I., B. M. Fonseca, N. Teixeira and M. D. Madeira (2016). "Induction and subcellular redistribution of progesterone receptor A and B by tamoxifen in the hypothalamic ventromedial neurons of young adult female Wistar rats." Mol Cell Endocrinol **420**: 1-10.

Saito, K., Y. He, X. Yan, Y. Yang, C. Wang, P. Xu, A. O. Hinton, Jr., G. Shu, L. Yu, Q. Tong and Y. Xu (2016). "Visualizing estrogen receptor-alpha-expressing neurons using a new ERalpha-ZsGreen reporter mouse line." Metabolism **65**(4): 522-532.

Sano, K., M. C. Tsuda, S. Musatov, T. Sakamoto and S. Ogawa (2013). "Differential effects of site-specific knockdown of estrogen receptor alpha in the medial amygdala, medial pre-optic area, and ventromedial nucleus of the hypothalamus on sexual and aggressive behavior of male mice." Eur J Neurosci **37**(8): 1308-1319.

Saunders, A., E. Z. Macosko, A. Wysoker, M. Goldman, F. M. Krienen, H. de Rivera, E. Bien, M. Baum, L. Bortolin, S. Wang, A. Goeva, J. Nemesh, N. Kamitaki, S. Brumbaugh, D. Kulp and S. A. McCarroll (2018). "Molecular Diversity and Specializations among the Cells of the Adult Mouse Brain." Cell **174**(4): 1015-1030.e1016.

Scalzo, R. L., R. M. Foright, S. E. Hull, L. A. Knaub, S. Johnson-Murguia, F. Kinanee, J. Kaplan, B. Freije, G. Verzosa, J. A. Houck, G. Johnson, A. M. Y. Zhang, J. D. Johnson, P. S. MacLean, J. E. B. Reusch, S. Wright-Hobart and E. A. Wellberg (2020). "Breast cancer endocrine therapy exhausts adipocyte progenitors promoting weight gain and glucose intolerance." bioRxiv: 2020.2008.2021.259440.

Shughrue, P. J., M. V. Lane and I. Merchenthaler (1997). "Comparative distribution of estrogen receptor-alpha and -beta mRNA in the rat central nervous system." J Comp Neurol **388**(4): 507-525.

Slee, P. H. T. J., D. De Vos, D. Chapman and D. Stevenson (1988). "The bioavailability of Tamoplex® (tamoxifen)." Pharmaceutisch Weekblad **10**(1): 22-25.

Starnes, L. M., C. M. Downey, S. K. Boyd and F. R. Jirik (2007). "Increased bone mass in male and female mice following tamoxifen administration." Genesis **45**(4): 229-235.

Stearns, V., L. Ullmer, J. F. Lopez, Y. Smith, C. Isaacs and D. Hayes (2002). "Hot flushes." Lancet **360**(9348): 1851-1861.

Takeo, T. and Y. Sakuma (1995). "Diametrically opposite effects of estrogen on the excitability of female rat medial and lateral preoptic neurons with axons to the midbrain locomotor region." Neurosci Res **22**(1): 73-80.

Turner, R. T., G. K. Wakley, K. S. Hannon and N. H. Bell (1988). "Tamoxifen inhibits osteoclast-mediated resorption of trabecular bone in ovarian hormone-deficient rats." Endocrinology **122**(3): 1146-1150.

van Veen, J. E., L. G. Kammel, P. C. Bunda, M. Shum, M. S. Reid, M. G. Massa, D. V. Arneson, J. W. Park, Z. Zhang, A. M. Joseph, H. Hrncir, M. Liesa, A. P. Arnold, X. Yang and S. M. Correa (2020). "Hypothalamic oestrogen receptor alpha establishes a sexually dimorphic regulatory node of energy expenditure." Nature Metabolism.

Vehmanen, L., I. Elomaa, C. Blomqvist and T. Saarto (2006). "Tamoxifen treatment after adjuvant chemotherapy has opposite effects on bone mineral density in premenopausal patients depending on menstrual status." J Clin Oncol **24**(4): 675-680.

Wade, G. N. and H. W. Heller (1993). "Tamoxifen Mimics the Effects of Estradiol on Food-Intake, Body-Weight, and Body-Composition in Rats." American Journal of Physiology **264**(6): R1219-R1223.

Waltman, L. and N. J. van Eck (2013). "A smart local moving algorithm for large-scale modularity-based community detection." The European Physical Journal B **86**(11): 471.

Watanabe, T., S. Inoue, S. Ogawa, Y. Ishii, H. Hiroi, K. Ikeda, A. Orimo and M. Muramatsu (1997). "Agonistic effect of tamoxifen is dependent on cell type, ERE-promoter context, and estrogen receptor subtype: functional difference between estrogen receptors alpha and beta." Biochem Biophys Res Commun **236**(1): 140-145.

Wilson, M. E., D. Mook, F. Graves, J. Felger, I. F. Bielsky and K. Wallen (2003). "Tamoxifen is an estrogen antagonist on gonadotropin secretion and responsiveness of the hypothalamic-pituitary- adrenal axis in female monkeys." Endocrine **22**(3): 305-315.

Windahl, S. H., G. Andersson and J. A. Gustafsson (2002). "Elucidation of estrogen receptor function in bone with the use of mouse models." Trends in Endocrinology and Metabolism **13**(5): 195-200.

Xu, Y., T. P. Nedungadi, L. Zhu, N. Sobhani, B. G. Irani, K. E. Davis, X. Zhang, F. Zou, L. M. Gent, L. D. Hahner, S. A. Khan, C. F. Elias, J. K. Elmquist and D. J. Clegg (2011). "Distinct hypothalamic neurons mediate estrogenic effects on energy homeostasis and reproduction." Cell Metab **14**(4): 453-465.

Ye, R., Q. A. Wang, C. Tao, L. Vishvanath, M. Shao, J. G. McDonald, R. K. Gupta and P. E. Scherer (2015). "Impact of tamoxifen on adipocyte lineage tracing: Inducer of adipogenesis and prolonged nuclear translocation of Cre recombinase." Mol Metab **4**(11): 771-778.

Yellen, G. (2018). "Fueling thought: Management of glycolysis and oxidative phosphorylation in neuronal metabolism." J Cell Biol **217**(7): 2235-2246.

Zhang, Z., J. Liu, A. G. Veldhuis-Vlug, Y. Su, E. Foppen, B. C. van der Eerden, M. Koedam, N. Bravenboer, A. Kalsbeek, A. Boelen, E. Fliers and P. H. Bisschop (2016). "Effects of Chronic Estrogen Administration in the Ventromedial Nucleus of the Hypothalamus (VMH) on Fat and Bone Metabolism in Ovariectomized Rats." Endocrinology **157**(12): 4930-4942.

Methods

Mice

All mice were maintained under a 12:12 h L/D schedule at room temperature (22 ºC ~ 23 ºC) and provided with food and water *ad libitum*. Mice expressing the NK2 homeobox transcription factor 1 (*Nkx2-1*; also known as *Ttf1*) Cre driver transgene (Tg(*Nkx2-1-Cre*)2Sand) and the *Esr1* floxed allele (*Esr1*tm1Sakh) were maintained on a CD-1;129P2 mixed background. We cross-bred mice carrying *Nkx2-1 Cre* with mice expressing *Esr1 flox* to generate ERα specific knock-outs in the hypothalamus. *Cre*-negative littermates were selected as controls. A total of 50 female mice were used. Mice were 8-10 weeks old at the start of the experiments. All studies were carried out in accordance with the recommendations in the Guide for the Care and Use of Laboratory Animals of the National Institutes of Health. UCLA is AALAS accredited and the UCLA Institutional Animal Care and Use Committee (IACUC) approved all animal procedures.

Tamoxifen administration

Tamoxifen (Sigma) was dissolved first in ethanol and then diluted in corn oil at a final concentration of 100 µg/mL and 0.5% of ethanol. Accordingly, the vehicle was prepared in corn oil containing 5% ethanol. We performed daily subcutaneous injection of tamoxifen at a dose of 0.1 mg/kg or an equal volume of vehicle control for 4 weeks. We estimated that this dose models human tamoxifen exposure based on studies of tamoxifen in human serum, estimates of total blood volume in mice, and bioavailability of tamoxifen delivered via subcutaneous injection*(Slee et al. 1988)*. Additionally, it is on the low end of what is used effectively in previous studies*(Wade and Heller 1993, Perry et al. 2005)*, which is desirable to minimize off-target effects.

Telemetry recording

Mice were anaesthetized with isofluorane and received combinatorial analgesics (0.01 mg/mL buprenorphine, 0.58 mg/mL carprofen) pre- and post- any surgeries. A G2 eMitter (Starr

748   Life Sciences) was implanted to the abdominal cavity and attached to the inside body wall of a

749   mouse. Mice were single-housed in cages placed on top of ER4000 Energizer/Receivers. Gross

750   movement and core body temperature were measured every 5 min using VitalView software

751   (Starr Life Sciences). These measurements were collected continuously for 3 days on and 3 days

752   off for the duration of the 28-day period. Telemetry data show 24-hour averages from the 2

753   telemetry sessions before and 3 weeks after tamoxifen or vehicle injections. Tail skin temperature

754   was monitored every 5 min using a Nano-T temperature logger (Star-Oddi) that was attached to

755   the ventral surface and 1 cm from the base of the tail in a 3D-printed polylactic acid collar modified

756   from Krajewski-Hall et al*(Krajewski-Hall et al. 2018)*. Tail skin data show 24-hour averages for the

757   same time periods as the telemetry data.

758   *Thermal imaging*

759   Infrared thermal images were captured using e60bx thermogenic camera (FLIR Systems)

760   and analyzed using the FLIR Tools software. All images were obtained at a constant distance to

761   subject in awake animals at light phase. BAT skin temperature was defined from the average

762   temperature of a spherical area centered on the interscapular region.

763   *Single-cell dissociation and library preparation*

764   To avoid circadian differences and batch effects, all four groups were performed in parallel

765   at the same time across 4 days with n=4 mice per day. Mice were euthanized two hours after the

766   last administration of tamoxifen or vehicle. The brain was freshly collected into ice-cold HABG

767   buffer (Fisher Scientific, Hampton, NH, USA) containing freshly prepared papain. A coronal

768   section containing the hypothalamus was quickly dissected along the boundary of rostral and

769   caudal spherical groves from the bottom of the brain. A third cut was made along the white fiber

770   of anterior commissure to get a square block of hypothalamic tissue (Figure 3 – Supplement 1A).

771   The hypothalamus tissue was then disassociated and prepared into a single-cell suspension at a

772   concentration of 100 cells/µl in 0.01% BSA-PBS using a previously described protocol *(Liu et al.*

773   *2020)*. Briefly, dissected tissues were incubated in a papain solution for 30 min at 30 °C then

774   washed with HABG. Using a siliconized 9-in Pasteur pipette with a fire-polished tip, the cells were

775   triturated carefully to help dissociate the tissue. Next, to separate the cells and remove debris,

776   the cell suspension was placed on top of a prepared OptiPrep density gradient (Sigma Aldrich,

777   St. Louis, MO, USA) then centrifugated at 800 g for 15 min at 22 °C. After debris removal, the cell

778   suspension containing the desired cell fractions was centrifugated for 3 min at 22 °C at 200 g, and

779   the supernatant was discarded. Finally, the cell pellet was re-suspended in 0.01% BSA (in PBS)

780   and filtered through a 40-micron strainer (Fisher Scientific, Hampton, NH, USA). The cells were

781   then counted and diluted to appropriate cell density.

782   Barcoded single cells, or STAMPs (single-cell transcriptomes attached to microparticles),

783   and cDNA libraries were prepared as described previously *(Liu et al. 2020)* and in line with the

784   online protocol v3.1 from McCarroll Lab (http://mccarrolllab.org/download/905/). Briefly, to

785   generate STAMPS, the prepared single cell suspensions, EvaGreen droplet generation oil (BIO-

786   RAD, Hercules, CA, USA), and ChemGenes barcoded microparticles (ChemGenes, Wilmington,

787   MA, USA) containing unique molecular identifiers (UMIs) and cell barcodes were co-flowed

788   through a FlowJEM aquapel-treated Drop-seq microfluidic device (FlowJEM, Toronto, Canada)

789   at recommended flow speeds (oil: 15,000 µl/h, cells: 4000 µl/h, and beads 4000 µl/h). After

790   breakage of the droplets, the beads were washed and suspended in reverse transcriptase solution.

791   Prior to PCR amplification, samples underwent an exonuclease I treatment. Next, the beads were

792   washed, counted and aliquoted into PCR tubes (6000 beads/tube) for PCR amplification (4+11

793   cycles). The cDNA quality was checked using a High Sensitivity chip on BioAnalyzer (Agilent,

794   Santa Clara, CA, USA) then fragmented using Nextera DNA Library Preparation kit (Illumina, San

795   Diego, CA, USA) with multiplex indices. The libraries were then purified, quantified, and

796   sequenced on an Illumina HiSeq 4000 (Illumina, San Diego, CA, USA).

797   *Analysis of single-cell RNA-seq*

798   Single cell transcriptomic data were analyzed in R version 3.6.1 using the package

799   "Seurat" version 3.2.0 and custom Seurat helper package "ratplots" version 0.1.0 written for this

800   study. All custom functions and complete analysis scripts are available at

801   https://github.com/jevanveen/. Cells were filtered for quality with the following criteria: cells

802   with > 15% of reads coming from mitochondrial genes were excluded and cells with fewer than

803   200 or more than 4000 genes detected were excluded. Samples derived from the four

804   experimental conditions: Wild-type, vehicle treated; Wild-type, tamoxifen treated; $Esr1^{cKO}$,

805   vehicle treated; and $Esr1^{cKO}$, tamoxifen treated, were aligned based on the expression of 2000

806   conserved highly variable markers in each group. Cells were clustered based on transcriptome

807   similarity, using a shared nearest neighbor algorithm *(Waltman et al. 2013)*. For each cell

808   cluster, marker genes were determined by comparing expression in the given cluster against all

809   other clusters using the smart local moving algorithm to iteratively group clusters together

810   *(Blondel et al. 2008)*. For all differentially expressed gene marker analyses, statistical

811   significance testing was performed with the Seurat default Wilcoxon rank-sum-based test and

812   Benjamini–Hochberg method for multiple-testing correction. Gene set enrichment analyses were

813   performed in R using the package "fgsea" version 1.14.0. GSEA analyses to find estrogen

814   signatures were done using the gene ontology pathway "GO_ESTROGEN_RESPONSE" taken

815   from mSigDB version 6.2. For general pathway analyses, a custom set of pathways was

816   assembled from mSigDB "Hallmark" pathways version 6.2 and selected GO pathways (version

817   6.2) particularly relevant to neural development and function. The complete list of these

818   pathways is given in Table S2.

819   Cells annotated as neurons were extracted and re-clustered using the same steps used

820   to cluster all cells, with the following differences: 500 highly variable genes were used to align

821   neurons from different treatment groups. No additional quality filtering was performed. Neuronal

822   sub-types were annotated based on top marker genes, defined as the highest logFC compared

823   to all other neuronal sub-types, whilst meeting the criterion of adjusted P value < .05. Gene set

824   enrichment analyses were performed on neuronal sub-types using the same gene sets and

825   methods performed for general cell types. All graphs and tables in figures 3-5 were produced

826   using the R packages "ggplot2" version 3.3.2 and custom functions in "ratplots" version 0.1.0.

827   *Micro-computed tomography*

828   Left femoral bones from the hind legs were dissected, cleaned of any soft tissue and frozen

829   in PBS at -20 °C till further analysis. Samples were scanned in 70% ethanol using Scanco Medical

830   μCT 50 specimen scanner with a voxel size of 10mm, an X-ray tube potential of 55 kVp and X-

831   ray intensity of 109 μA. Scanned regions included 2 mm region of the femur proximal to epiphyseal

832   plate and 1 mm region of the femoral mid-diaphysis. For the analysis, a trabecular bone

833   compartment of 1mm length proximal to the epiphyseal plate was measured. Cortical parameters

834   were assessed at the diaphysis in an adjacent 0.4 mm region of the femur. In both specimen and

835   in vivo scanning, volumes of interest were evaluated using Scanco evaluation software.

836   Representative 3D images created using Scanco Medical mCT Ray v4.0 software.

837   *Immunohistochemistry*

838   Mice were perfused transcardially with ice-cold PBS (PH=7.4) followed by 4%

839   paraformaldehyde (PFA) in PBS. Brains were post fixed in 4% PFA overnight, dehydration in 30%

840   sucrose for 24 hours, embedded in OCT and stored in -80 °C before sectioning. Coronal sections

841   were cut under cryostat (Vibratome) into 8 equal series at 18 μm. ERα immunoreactivity was

842   detected using hot based antigen retrieval immunohistochemistry protocol. Briefly, sections were

843   first incubated in antigen retrieval buffer (25 mM Tris–HCl, 1 mM EDTA, and 0.05% SDS, pH 8.5)

844   at 95 °C for 40 min. Sections were then blocked for 1 h in 10% BSA and 2% normal goat serum

845   (NGS) and incubated overnight at 4 °C with primary antibody (ERα, 1:250, sc-8002, Santa Cruz).

846   Following 3 X 10 min washing in PBS, sections were incubated with Fluorophore conjugated goat

847   anti-mouse secondary antibody (Thermo Fisher Scientific) for 2 h at room temperature. After

848   washing, section were incubated with DAPI, PBS washed and coverslipped with Fluoromount-G.

849   The images were taken by DM1000 LED fluorescent microscope (Leica).

850   Cyan/magenta/yellow pseudo-colors were applied to all fluorescent images for color-friendly

851   accessibility. Image processing was performed using the Leica Application Suite (Leica) and

852   ImageJ (NIH).

853   *RNA isolation and Real Time PCR (qPCR)*

854   Interscapular BAT was snap frozen in liquid nitrogen and stored at -80 ºC until analysis.

855   Total RNA from BAT was isolated using Zymo RNA isolation kit (ZYMO Research) and RNA yield

856   was determined using a NanoDrop D1000 (Thermo Fisher Scientific). cDNA synthesis was

857   performed with equal RNA input using the Transcriptor First Strand cDNA synthesis kit (Roche

858   Molecular Biochemicals). Quantitative PCR was performed using C1000 Touch Thermal Cycler

859   (BioRed) and SYBR mix (Bioline, GmbH, Germany), using validated primer sets *(Herber et al.*

860   *2019)* (Table 1).

861   **Statistics**

862   Data are represented as mean ± standard error of the mean (SEM). Data with normal

863   distribution and similar variance were analyzed for statistical significance using two-tailed,

864   unpaired Student's t-tests. Time course data were analyzed by repeated measures two-way

865   ANOVA or mixed model followed by Sidak's multiple comparisons. Significance was defined at a

866   level of $P < 0.05$. Statistics were performed using GraphPad Prism 8 and RStudio.

867